3-2020

HeartQuake: Accurate low-cost non-invasive ECG monitoring using bed-mounted geophones

Jaeyeon PARK

Hyeon CHO

Rajesh Krishna BALAN
Singapore Management University, rajesh@smu.edu.sg

JeongGil KO

HeartQuake: Accurate Low-Cost Non-Invasive ECG Monitoring Using Bed-Mounted Geophones

JAEYEON PARK, School of Integrated Technology, Yonsei University, South Korea
HYEON CHO, Department of Computer Engineering, Ajou University, South Korea
RAJESH KRISHNA BALAN, School of Information Systems, Singapore Management University, Singapore
JEONGGIL KO*, School of Integrated Technology, Yonsei University, South Korea

This work presents *HeartQuake*, a low cost, accurate, non-intrusive, geophone-based sensing system for extracting accurate electrocardiogram (ECG) patterns using heartbeat vibrations that penetrate through a bed mattress. In *HeartQuake*, cardiac activity-originated vibration patterns are captured on a geophone and sent to a server, where the data is filtered to remove the sensor's internal noise and passed on to a bidirectional long short term memory (Bi-LSTM) deep learning model for ECG waveform estimation. To the best of our knowledge, this is the first solution that can non-intrusively provide *accurate ECG waveform characteristics* instead of more basic abstract features such as the heart rate using bed-mounted geophone sensors. Our extensive experimental results with a baseline dataset collected from 21 study participants and a longitudinal dataset from 15 study participants suggest that *HeartQuake*, even when using a general non-personalized model, can detect all five ECG peaks (e.g., P, Q, R, S, T) with an average error of 13 msec when participants are stationary on the bed. Furthermore, clinically used ECG metrics such as the RR interval and QRS segment width can be estimated with errors 3 msec and 10 msec, respectively. When additional noise factors are present (e.g., external vibration and various sleeping habits), the estimation error increases, but can be mitigated by using a personalized model. Finally, a qualitative study with 11 physicians on the clinically perceived quality of *HeartQuake*-generated ECG signals suggests that *HeartQuake* can effectively serve as a screening tool for detecting and diagnosing abnormal cardiovascular conditions. In addition, *HeartQuake*'s low-cost and non-intrusive nature allow it to be deployed in larger scales compared to current ECG monitoring solutions.

CCS Concepts: • **Human-centered computing** → **Ubiquitous and mobile computing systems and tools**; • **Computer systems organization** → *Embedded and cyber-physical systems.*

Additional Key Words and Phrases: ECG Waveform Prediction, Contactless Physiological Sensing

ACM Reference Format:
Jaeyeon Park, Hyeon Cho, Rajesh Krishna Balan, and JeongGil Ko. 2020. HeartQuake: Accurate Low-Cost Non-Invasive ECG Monitoring Using Bed-Mounted Geophones. *Proc. ACM Interact. Mob. Wearable Ubiquitous Technol.* 4, 3, Article 93 (September 2020), 28 pages. https://doi.org/10.1145/3411843

*Corresponding Author: jeonggil.ko@yonsei.ac.kr

Authors' addresses: Jaeyeon Park, School of Integrated Technology, Yonsei University, 85 Songdogwahak-Ro, Yeonsu-Gu, Incheon, South Korea; Hyeon Cho, Department of Computer Engineering, Ajou University, 206 Worldcup-Ro, Yeongtong-Gu, Suwon, South Korea; Rajesh Krishna Balan, School of Information Systems, Singapore Management University, 80 Stamford Road, Singapore; JeongGil Ko, School of Integrated Technology, Yonsei University, 85 Songdogwahak-Ro, Yeonsu-Gu, Incheon, South Korea.

2474-9567/2020/9-ART93 $15.00
https://doi.org/10.1145/3411843

1 INTRODUCTION

Statistically, a significant fraction (over 48%) of the U.S. population above the age of 18 will develop some heart-related condition ranging from arrhythmia to life threatening myocardial infarction (i.e., heart attack), etc. [16, 17, 52, 61, 97]. These conditions could cause major quality of life issues that include loss of mobility, loss of speech, and even loss of life. The cost, both in terms of personal welfare and healthcare expense, due to cardiac disorders is estimated to be in the trillions [9, 17, 31]. Thus, it is vital to detect these conditions as early as possible to improve the chances of recovery. However, these heart conditions could be either intermittent (e.g., arrhythmia) or instantaneous (e.g., heart attack) and any sensing techniques used must be both accurate and continuous enough to detect both cases.

There are numerous smartwatches and other wearable devices that can measure the heart rate (in beats per minute) of an individual in fairly unobtrusive ways [11, 13, 24, 28, 66, 77, 91]. However, the heart rate, alone, is insufficient for detecting many serious heart conditions, which include various forms of arrhythmia and heart block [48, 62, 80, 82, 83]. To accurately diagnose and detect such emergencies, electrocardiogram (ECG) signals are widely used, as they contain detailed temporal information about the workings of the heart.

To emphasize this point, Table 1 shows nine commonly occurring abnormal cardiovascular conditions along with the sensing modality needed to reliably detect each condition. In particular, notice that much more than simple heart rate information is needed to detect these conditions. Even more advanced heart rate variability (HRV) measurements are insufficient for the majority of the ailments. Hence, having continuous and reliable ECG sensing is important to detect heart conditions and can be a true life saver in many situations.

However, deploying ECG sensors among the general population is not easy for two primary reasons: (1) clinical grade ECG sensors are very expensive. For example, ECG monitoring devices used in hospital intensive care units (ICUs) cost between USD$10,000 to 30,000 [18, 72]. This makes clinical grade sensors much too expensive to widely deploy. (2) Mass market ECG sensors [41, 76, 87, 114] require either a tight band to be wrapped around the chest or electrodes to be stuck at specific places on the body. Neither option is easy nor comfortable enough to be used constantly – especially while sleeping.

In this paper, we focus on detecting *ECG signals* continuously, accurately, and non-intrusively while a person is sleeping, and propose a solution, called *HeartQuake*, that overcomes the limitations of current approaches designed to be used while sleeping. Specifically, *HeartQuake* does not involve any body-attached sensors and exploits a geophone sensor attached to the bed's mattress to detect cardiac activity patterns of the bed's occupant. We focus on sleep sensing as this is a particularly crucial sensing period for many reasons; (1) the person is unaware when issues occur and thus may go untreated for hours, (2) most people spend up to 7 or 8 hours sleeping – a significant fraction of their time, and (3) existing more invasive sensing methods, such as chest straps etc., that may be suitable while awake will not work well while sleeping (due to the discomfort).

There have been previous approaches that use bed-attached geophone sensors to implicitly understand cardiac activities. However, they can only detect the heart rate [46, 47] (in beats per minute). As stated earlier, this is insufficient for detecting many common heart ailments. As far as we know, *HeartQuake* is the first geophone-based solution that can capture all five core ECG peaks (P, Q, R, S, and T-peaks), making it a much more accurate solution for diagnosing various heart conditions.

HeartQuake achieves this by exploiting the fact that the geophone attached to the bed is essentially a seismography sensor – i.e., it can detect the intensity, direction, and duration of anything that makes the bed move (even minute motions). Thus, it can be used to capture vibrations that the bed occupant's heart pulse generates, similar to a seismocardiography (SCG) signal. From prior work [89], we know that ECG and SCG signals are loosely correlated. Therefore, we construct an inference model that uses the vibration signal to estimate the corresponding ECG waveforms. This work is the first work to estimate accurate ECG patterns using a geophone

Table 1. Types of abnormal cardiovascular conditions with their prevalence, and detection feasibility using heart rate, heart rate variability and ECG. Note: "Screening Only" for HRV indicates that HRV cannot be used to concretely diagnose the condition, but can be used for initial screening.

Abnormal Condition	Prevalence per 100,000 persons (age range)	Heart Rate (HR)	Heart Rate Variability (HRV)	Electrocardiogram (ECG)	Factors needed from ECG signal for detection	PPG-based smart watch	*HeartQuake*
Arrhythmia - Ventricular Fibrillation [9]	127 (≥18)	✓	✓	✓	R peak	✓	✓
Arrhythmia - Atrial fibrillation [50]	965 (≥65)		✓ (Screening Only)	✓	RR interval, QRS complex, P and T peaks	✓ (Screening Only)	✓
Arrhythmia - Bradyarrhythmia [50]	286 (≥65)		✓ (Screening Only)	✓	RR interval, PR interval, PR segment, P peak	✓ (Screening Only)	✓
Arrhythmia - Atrial flutter [9]	36 (≥60)		✓ (Screening Only)	✓	RR interval, QRS complex, P peak	✓ (Screening Only)	✓
Arrhythmia - Supraventricular tachycardia [9]	616 (≥65)			✓	RR interval, QRS complex P peak		✓
Arrhythmia - Ventricular tachycardia [50]	157 (≥65)			✓	RR interval, QRS complex, PQ interval		✓
Heart Block - Atrioventricular node block [9]	56 (≥40)			✓	RR interval, QRS complex PR segment		✓
Ectopic Heart Beat - Premature ventricular contraction [9]	0.011% of all beats (≥65)			✓	RR interval, QRS complex, P peak		✓
Ectopic Heart Beat - Premature atrial contraction [23]	8.2% of all beats (≥50)			✓	RR interval, QRS complex, P peak		✓

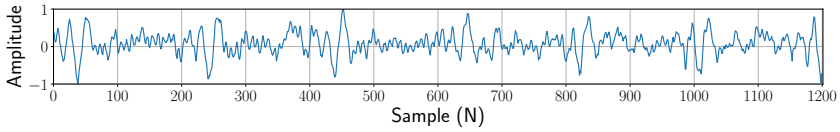

(a) Raw vibration captured from a bed-attached geophone

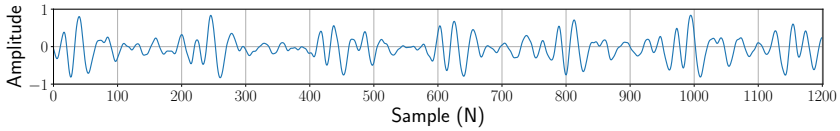

(b) Vibration signals after filtering - containing heart pulse vibrations

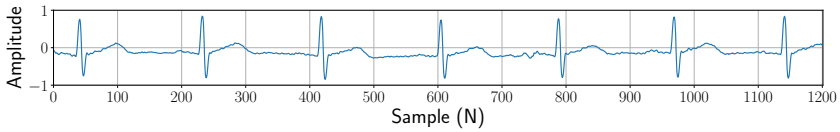

(c) Estimated ECG using *HeartQuake*

Fig. 1. Waveforms used and generated in *HeartQuake*.

sensor on the bed. While previous works successfully extract abstract forms of cardiac activity [46, 47, 105], estimating accurate ECG features require a much more complex system design.

In particular, *HeartQuake* uses a bidirectional long short-term memory (Bi-LSTM)-based deep learning model for converting vibration signals into ECG feature estimations. Figure 1 shows an example of how *HeartQuake* works, and plots the raw vibrations from the bed (Fig. 1 (a)), the filtered vibration signal (Fig. 1 (b)) and the estimated ECG from *HeartQuake* (Fig. 1 (c)).

For designing and evaluating *HeartQuake*, we constructed a baseline dataset by collecting geophone vibration patterns and ground truth ECG samples from 21 participants through an IRB approved study. Our evaluations showed that the average timestamp estimation accuracy of all five ECG peaks is 13.26 msec with a general model and 9.37 msec with a personalized model, with the R-peak estimation showing only 6.66 msec of error compared

to a ground-truth ECG (from an FDA-approved Zephyr Bioharness chest strap sensor). Moreover, when observing the performance of *HeartQuake* using clinically used ECG features, *HeartQuake* shows an RR interval estimation error of <3 msec, and the QRS complex width estimation error of <10 msec. We also evaluated *HeartQuake* with a longitudinal study, in which we gathered bed vibration and ECG ground truth data from 15 participants for at least 2 hours each while they are sleeping, summing up to a total of 71 hours of data. Results from this dataset also showed low average peak estimations errors of 15.83 msec with a general model and 8.50 msec with model personalization. Furthermore, we present detailed micro benchmarks (e.g., varying sensor locations, external vibrations, motion and posture, different mattress types) showing the robustness of *HeartQuake* under practical usage scenarios.

Finally, we also performed a qualitative study with 11 clinical doctors (avg. 10+ years of practice; currently practicing at six different university hospitals) to compare the quality of authentic and *HeartQuake*-generated ECG waveforms. Results from this study indicates that doctors could properly identify abnormalities from *HeartQuake*-generated ECG waveforms, and that these signals were difficult to distinguish from ECG waveforms collected from body-attached medical-grade sensors. Overall, our extensive evaluations reveal that *HeartQuake* is accurate enough to serve as a first-level screening tool that triggers detailed clinical examinations when needed.

Specifically, this paper makes the following contributions.

- We show that the vibration signals of a person lying by a mattress can be captured by a geophone attached to the mattress and transformed into vibration patterns similar to SCG signals. We then show that these waveforms can be used to accurately estimate ECG patterns and that producing an accurate ECG signal is a much more complicated task than just detecting the heart rate of a person.
- We present *HeartQuake*, a low-cost (~$100) system that can accurately estimate a person's ECG patterns using just a mattress-attached geophone sensor (no sensors attached to the person at all) by combining a filtering process on the vibration data with a Bi-LSTM-based deep learning model. *HeartQuake* is, to the best of our knowledge, the first solution to translate heart-generated vibration data into accurate ECG signals.
- We show, using both open datasets and an IRB-approved study with 36 participants (21 in a baseline study and 15 in a longitudinal study), that *HeartQuake* can accurately estimate the most important ECG waveform components (i.e. the ones used for clinical diagnosis).
- Finally, we show, via a qualitative study with 11 medical specialists who use ECG data daily (4 cardiologists, 2 emergency medicine specialists, 3 infectious disease specialists, and 2 traumatologists), that *HeartQuake* produces results that are (a) indistinguishable from medical grade ECG data, and (b) useful for diagnosis purposes.

2 BACKGROUND AND MOTIVATION

2.1 Measuring Cardiac Activity

Clinical staff try to understand a patient's cardiac activity status using various sensing methodologies. Specifically, the following four types of body-attached sensors are widely used – electrical, seismic, acoustic, and optical.

1. Electrical signals - Electrocardiography (ECG): ECG measurements offer five important peak information along with other clinically crucial metrics that can be used to understand cardiac activity via electrical signals generated from the heart [19]. The ECG peak data, namely the P, Q, R, S, and T-peaks, form the basis of understanding how cardiac activities take place and can be used to capture various cardiac disorders such as myocardial infarction and arrhythmia [57] (full details in Table 1).

2. Seismic signals - Seismocardiography (SCG): The SCG captures vibrations generated from heart motions and blood flow [112] measured through body-attached seismic sensors to allow for a better understanding of the cardiac mechanics [99]. SCG measurements are made via sensors such as accelerometers, gyroscopes or

geophones attached to the body, but are sensitive to the installation orientation; thus, are not typically used alone for diagnosis. Nevertheless, SCG measurements are often used to assist ECG measurements in quantifying their reliability [85, 110].

3. Acoustic signals - Phonocardiography (PCG): PCG is a signal captured using a transducer that converts vibration into acoustic signals. In particular, this sensor is used to identify abnormalities in the cardiac valves and understand cardiac valve activity [27]. PCG measurements provide more in-depth acoustic data generated from the heart compared to a stethoscope, which includes cardiac murmurs for a better understanding of cardiac functional activities.

4. Optical characteristics - Photoplethysmography (PPG): When using PPG, different wavelengths of light emitted from light emitting diodes (LEDs) illuminate the phosphor parts of the body to detect changes in light reflections as blood passes through the veins. PPG measurements are used to measure the heart rate via minimally invasive sensor attachments [7]. This sensor is commonly used on smartwatches and finger tip sensors due to its small form factor. However, external lighting conditions and motion artifacts make it challenging to accurately capture PPG measurements. In order to solve such problems, non-contact (remote) PPG schemes have recently been proposed to monitor heart rate variability (HRV) using webcams [53, 56, 73, 115], or the smartphone's front camera [39, 54].

These different signals each characterize cardiac activities in different dimensions to offer a comprehensive view for diagnosis. Among these, the most detailed measurements commonly used by cardiologists are ECG signals. Unlike simple heart rate measurements, which can be captured from easily accessible wearable platforms, ECGs allow for a much deeper understanding of various cardiac abnormalities [8, 43, 113]. For this reason, cardiologists use the ECG signal patterns along with their P, Q, R, S, and T peak information to make various diagnosis related to cardiac activities [42]. However, capturing ECG is a cumbersome process as it involves attaching a number of sensors to the human body. Thus, a system that captures accurate ECG signals non-intrusively can be very useful for many clinical applications.

2.2 Motivating Scenarios

All of the aforementioned metrics, especially ECG, provide important information for clinical decision making. However, they all require special sensors to be attached to the human body. While these sensors are installed near each bed in urgent care units (e.g., ICUs), general wards, where most patients are treated, do not have such devices persistently installed. There are many reasons for this with the dominant reason being the high cost of the sensing devices. A clinical-grade ECG monitor used at major hospitals can cost from $10,000-$30,000 or even more. Having such a device at each bed, given that large hospitals host thousands of bed units, can significantly increase healthcare costs. In addition, these monitors use multiple body attached sensors and are uncomfortable to use if not absolutely needed. Thus, for the majority of general ward patients, due to cost and comfort reasons, physiological signal monitoring only occurs a few times a day and is done manually by nurses during their rounds. To make things worse, there is no monitoring during the night in many cases as the concern is that taking measurements can interfere with the patients' sleeping patterns. Unfortunately, there is a need for monitoring, even at night, as there are enough reports of patients, in general wards, who experience sudden deterioration in cardiac conditions overnight [22, 67, 68, 81].

In addition, similar issues arise for patients that were discharged from the hospitals and transferred as out-patients or even for regular individuals who may be at risk of cardiac issues. As they sleep at home, instantaneous health deterioration cannot be monitored (nor self-reported) due to the lack of monitoring infrastructure. While Holter monitors can offer continuous ECG monitoring [59], providing each patient with a Holter monitor is not considered effective, due to price (e.g., Philips DigiTrak ($2,700) [29], GE healthcare SEER 1000 ($2,000) [1], Medtronic LINQ ($4,000) [63], etc.) and usability limitations (i.e., multiple wired leads need to be continuously

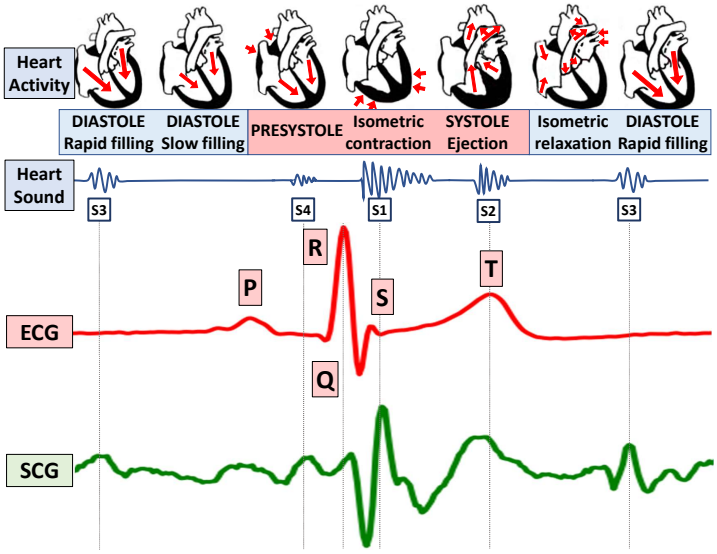

Fig. 2. A sample relationship between ECG and SCG for the b013 record from the CEBS dataset.

attached to the body). Mass market ECG sensing platforms, typically in the form of chest strap devices (e.g., Qardio QardioCore ($400) [76], Zephyr Bioharness ($600) [2], etc.), can be alternatives to Holter monitors, but they also cause cumbersomeness, leading to usability issues when attached continuously to a person's body. Finally, smartwatch or similar type devices cannot continuously sense ECG signals; instead they just provide heart rate information which is insufficient for detecting many cardiac conditions (Table 1).

These scenarios motivate the need for monitoring a person's ECG in a cost-effective and non-intrusive way. Specifically, a low-cost platform that can (at the very least) act as a screening tool to identify urgent patients that need immediate attention or further examination can enable a number of life-saving applications.

2.3 Capturing ECG from Vibration

This work presents a solution to non-intrusively capture the ECG of a bed's occupant using vibrations generated from heart activities. With filters applied to the vibrations, we extract signals that share similar characteristics with an SCG, which then is "translated" to ECG signals. This section discusses how such a translation between the two heterogeneous signals can be possible.

We note once more that, fundamentally, the SCG is in the form of vibration signals generated from the heart. Thus, we try to understand how cardiac vibrations can be translated to ECG using SCG signals as an example.

Both SCG and ECG are time-series traces collected from a person's heart: SCG represents the seismic vibrations caused by periodic cardiac motion and blood flow, while ECG shows the corresponding electric signals. From this observation, the two are (potentially) closely correlated, since, from a clinical stand-point, electrical activities cause periodic de-polarization and re-polarization of the heart, resulting in periodic cardiac muscle contraction, relaxation, and blood flow. Figure 2 shows an example of how cardiac activities impact the two different signals.

From the Figure 2, we observe that the P, Q, R, S, and T peaks[1] of the ECG signals are generated by the electrical activity of the heart, and are temporally-correlated with four core heart sounds $S1$, $S2$, $S3$, and $S4$ in Figure 2, which are also captured in the SCG. In detail, the core heart sounds consist of the first heart sound $S1$ (mitral

[1]P and T regions are often denoted as "slopes" or "waves" in the literature, but we use the term "peaks" to indicate the highest point on each slope.

valve closing sound, a valve between the left atrium and left ventricle), the second heart sound $S2$ (aortic valve closing sound, a half-moon valve connecting the ventricles and the large blood vessels), the third heart sound $S3$ (adventitious sound caused by rapid filling), and the fourth heart sound $S4$ (gallop rhythm in the process of arterial presystole). These sounds are caused by the electrical activity (ECG) of the heart.

In addition to the core sounds, there is also heart murmur, the noise generated inside and outside of the heart, including both physiological and pathological sounds from the obstruction of blood flow due to the stenosis and valve failures. These activities generate vibration and are comprehensively mixed and reflected in SCG signals. The potential correlation between the two signals is the core observation we exploit when designing our system, *HeartQuake*, using externally collected vibration signals (which embed the SCG waveform with other noise factors) to recover the ECG waveform.

It is important, however, to note that while Figure 2 presents a nice example of SCG to ECG correlation, the different noise artifacts included in an SCG signal and also the complexity of the signal itself, makes the formulation of a direct one-to-one mapping of the two difficult. While there have been many studies to correlate these signals accurately, a precise time-scale correlation between the two is still unknown, even in the clinical research domain [49, 58, 102]. Thus, *HeartQuake* is, to the best of our knowledge, a novel solution to translate heart-issued vibration data into accurate ECG signals.

3 *HEARTQUAKE*

HeartQuake is designed to satisfy the requirements stated in the earlier sections; namely to accurately estimate a person's ECG waveform using a cheap non-intrusive geophone sensor installed under the mattress of the bed. Specifically, the geophone sensor captures the vibration patterns that a person's heart injects through the mattress and our system uses a band-pass filter to eliminate the internal noise that the sensor itself introduces. Next, from the observation that there is some relationship between the heart's vibration and ECG signals, we train a deep learning model with vibration and ECG signal pairs to implement a system capable of estimating a person's true ECG waveform from bed-collected vibration signals.

Specifically, the design goals of *HeartQuake* are as follows:

- The system should involve no sensor attachments directly to the human body for capturing ECG signals.
- The system should be able to provide sufficiently accurate ECG waveforms and not just simple heart rate information to be effective enough for use as a screening tool prior to detailed clinical examinations.
- The cost of system installation should be kept low to enable large-scale hospital and at-home deployments.

Overall, the goal of *HeartQuake* is to build a fully non-intrusive, cheap, yet effective system for capturing ECG signals from a bed's occupant. We first provide an overview of *HeartQuake*'s core components: the hardware, the signal filter, and the ECG estimation module, and also present how these components are integrated to form a full working prototype system.

3.1 Hardware Components

HeartQuake relies on a geophone sensor attached to the bed's mattress on which the observation subject lies. The geophone, which usually consists of a coil, magnet, and two springs at the top and bottom, measures the amount of vibration in the environment using the inertial mass suspended from the springs [37]. Specifically, in *HeartQuake* we use the SM-24 geophone sensor, which is a widely used sensor for environmental seismic sensing [5, 6, 70]. The sensor offers a sensitivity of 28.8 V/m/s and captures reliable measurements for the 0.5 to 50 Hz frequency range at a low-cost [4, 94]. The geophone is attached to a mattress' top panel while avoiding interference with sleep habits but capturing the most heart vibrations of the sleeping user. It produces 10 kHz raw analog sensor signals that are first amplified through its own amplifier circuit with an amplification gain

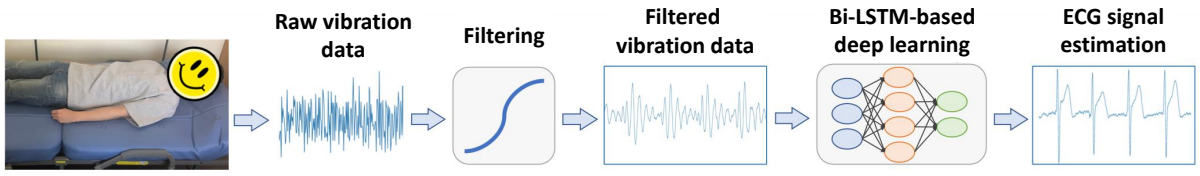

Fig. 3. Overall operational flow of *HeartQuake*.

of 90 *dB* and digitalized by a Raspberry Pi 3 B+ [78] to obtain fine-grain measurements of the sleeping user's vibration patterns. Note that in this work even for different mattress, these configurations were kept the same.

Based on hardware components, the estimated cost for this platform is less than $100. This makes *HeartQuake* affordable for large-scale deployments in hospitals and at homes for patients that require remote monitoring. Note: current clinical-grade ECG monitoring solutions for hospitals cost more than $10,000 [18, 72] or more and require invasive probes connected directly to the body and accurate chest strap-based wearables cost more than $400 [41, 76, 87, 114].

3.2 Signal Filtering

While the geophone sensor is sensitive enough to capture the heartbeat-generated vibrations from the bed, unfortunately, due to physical limitations of the sensor itself, the sensor introduces a noticeable amount of internal noise. Thus, there is a need to understand the internal noise patterns of the sensor and eliminate as much of this noise as possible to leave only the human-generated patterns in the vibration. We explain in Section 4 how we implemented a band-pass filter that suppresses such frequency domains in which noise patterns are dominant. Figure 3 presents an operational overview of *HeartQuake*'s workflow including this noise filtering process.

3.3 ECG Waveform Estimation

HeartQuake uses the filtered vibration data to estimate the corresponding ECG signals. However, as there is no simple way to transform heart-generated vibration signals into ECG [100], applying signal processing methods to directly translate the filtered vibration signals to ECG signals is not possible. Instead, we exploit the underlying features inherent in the vibration signals [85] to train a deep learning model with simultaneously collected vibration and ECG data such that vibration signals used as inputs will output an ECG waveform that matches the input signal. Given that the vibration signals generated from a person's heart shows a complex signal pattern (i.e., more than clinically-meaningful 20 feature points embedded in the signals [98, 100]) the main challenge in designing a deep learning model for predicting ECG from these vibrations is caused from the variations of the signals' morphology due to natural cardiovascular vibrations and inter-subject variations. Even in the clinical domain, mapping the ECG signal with heart-generated vibrations is still an area of on-going research [38, 90, 106, 107, 111].

When designing the deep learning model for this purpose, we use the fact that both the input and output datasets used in *HeartQuake* are time-series data which naturally fits a recurrent neural network (RNN) architecture. RNNs, a class of artificial neural networks for learning the temporal sequence of a data by processing a sequence of inputs using its internal states consisting of cells, are widely used in applications with sequential input data [10, 35, 86]. Among various RNN options, *HeartQuake* applies the bi-directional long short term memory (Bi-LSTM) architecture, which combines a forward LSTM and a backward LSTM to further emphasize on the sequential characteristics of the vibration and ECG data [88]. In detail, while LSTMs are capable of learning the long time dependencies [33, 35], baseline LSTMs cannot fully utilize the future input information in a sequence,

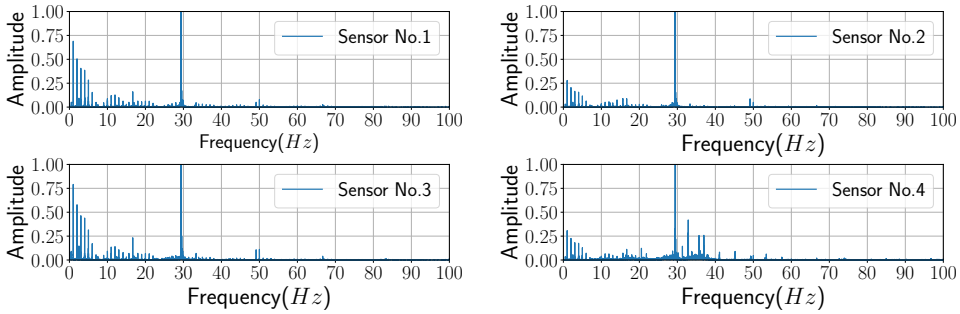

Fig. 4. Internal noise patterns observed from four SM-24 sensors in idle environments.

which usually also contains meaningful information. To overcome this fundamental limitation of baseline LSTMs, we select to use Bi-LSTMs that can leverage both past and future information within a frame's sequence. Thus, considering that the filtered vibration data consists of at least two or more signals, we train our model to learn the sequence of the data points within each signal as well as the sequence of the patterns *among* the signals. From this inference model, the mattress-collected vibration signals can be used to estimate the corresponding ECG patterns. We explain the detailed network architecture design and its specific parameters in Section 5.

3.4 Overall System Integration

Overall, the geophone used by *HeartQuake* is installed under the bed's mattress. The bed can be located within the hospital or at a person's home and we assume that any bed deployment has a stable Internet connection and a consistent power supply. Hence, we do not need to design a low-power low-bitrate solution, and the vibration samples collected at the geophone are streamed to a backend server via WiFi where the samples to be thoroughly analyzed. At the server, the vibration samples are filtered and provided as input to the ECG estimation Bi-LSTM deep learning model, which outputs a estimated ECG pattern. *HeartQuake* outputs the ECG waveforms themselves as well as different clinical metrics (e.g., timestamps for P, Q, R, S, T-peaks, RR interval, QRS segment length, etc.) that can be extracted from the ECG.

4 GEOPHONE DATA FILTERING

When deploying a sensor system, one important aspect to consider is the internal noise introduced by the sensor. This internal noise can impact all samples collected from the sensor, which in turn, can affect the quality of the final ECG estimation from our model. Therefore, the primary purpose of this filter is to remove the persistent internal noise that the sensor itself introduces.

To do so, we first start with an analysis of the internal noise patterns of our target geophone device. In this work, we use the SM-24 device and in Figure 4 we present the Fast Fourier Transform (FFT) results obtained from four of these devices located in different idle locations with no external motion/vibrations. Figure 4 suggests that the samples from all four sensors show a similar pattern: with noticeable noise in the frequency range of 0-5 Hz, smaller amounts of noise in the 10-20 Hz range, a high noise peak near 30 Hz and just minor noise scatters beyond the 30 Hz range. Ideally, if these frequency ranges do not interfere with the vibrations generated by a user's heartbeat, we can use a set of band pass filters to de-noise the geophone's output signals.

To understand whether and how this noise would impact our results, we used data from the CEBS dataset in PhysioNet [15] that contains clinical grade time-correlated ECG and SCG data for 20 subjects, summing up to 1,200 minutes of data for each signal type. Using the dataset's SCG samples (which again, are heart-generated vibration

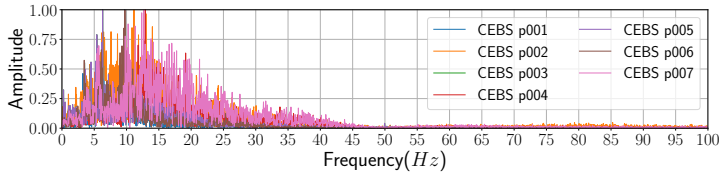

(a) FFT results for CEBS SCG data

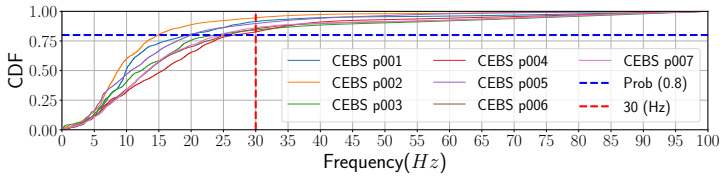

(b) CDF of frequency distributions

Fig. 5. FFT of SCG data for seven subjects with CDF of signal distribution over different frequencies.

signals themselves), we performed FFTs, shown in Figure 5(a), for seven subjects (the other 13 showed similar patterns) to understand the distribution of frequencies embedded in these SCG waveforms. We observe that the most prominent vibration frequency range is in the 5 to 30 Hz range, which agrees with similar observations made in previous work [14, 45, 103]. Quantitatively, the CDFs for these frequencies are plotted in Figure 5(b) and confirm that the frequency range between 5-30 Hz contains more than 80% [44] of the signal embedded in the waveforms. Hence, we conclude that the core frequency band of SCG data, which needs to be extracted from our raw vibration signals, is in the 5-30 Hz range. We emphasize that while a person's typical heartbeat is in the range of $<5Hz$, in this work we focus on the different signal frequency characteristics that are embedded within the SCG/vibration signal (e.g., heart valves, heart systole and diastole, blood filling and ejection, etc.) which mostly generate signals in the 5-30 Hz range.

We thus pre-process the incoming vibrations (from the geophone) by passing the signals through a band-pass filter that removes everything except the 5-30 Hz range. This removes the majority of the sensor's internal noise while preserving the vibration signal needed to identify the ECG. In addition, filtering signals below 5 Hz also allows our filter to eliminate the patterns caused from respiration, which is, in all cases, an added factor to the heart's beating vibrations.

We note that this simple filter design holds two major limitations. First, the filter is designed only for a specific sensor device. While we were able to validate that different SM-24 sensors have similar internal noise patterns, when using a different geophone sensor, different noise characteristics may be observed. Nevertheless, this can be addressed by understanding the characteristics of the new sensor through the same process as well. This is a one-time process and we do not see this as a practical issue when platforms such as ours are deployed operationally. The second limitation is that we cannot "perfectly" remove the internal sensor noise. As shown in Figure 4, despite filtering out signals in the <5 and >30 Hz range, there is still some noise in the non-filtered region as well (in the 10-20 Hz range). Fortunately, the relative amplitude of the noise is small compared to the true signal; allowing our deep learning model, presented in the next section, to still perform well.

5 BI-LSTM FOR ECG ESTIMATION

5.1 Data for Designing the Neural Network

The data used to build our deep learning model comes from two datasets: (1) a self-collected baseline dataset of mattress vibration data with ground truth ECG signals, and (2) the SCG and corresponding ECG data from the

CEBS dataset [15]. As briefly mentioned, the CEBS dataset is collected from 20 subjects (12 male, 8 female; ages 20-30), and contains SCG and time-synchronized ECG data collected using the clinical grade Biopac MP36 sensor [65] for 60 minutes per subject. Given that this dataset contains SCG data and its corresponding ground-truth ECG samples, it is a perfect fit for our purposes of estimating ECG from heart-generated vibration data.

For our self-collected dataset, we gathered mattress vibration patterns using the *HeartQuake* hardware and filtered the data as described in Section 4. Our baseline dataset was collected from 21 subjects (18 male, 3 female; ages 22-36) for 10 minutes per subject. All subjects were asked to lie down on a foldable couch-type bed during data collection. While gathering vibration data, we also collected synchronized ground-truth ECG signals using an FDA-approved Zephyr Bioharness 3 chestband [114]. We note that the data collection and experiments presented in this work were IRB-approved.

For data collection, the geophone sensor was positioned at the participant's left shoulder location below the mattress' top panel. This was to assure close proximity with the subject's heart location. For this dataset, we asked each participant to lay still while facing up. Even so, the vibration data still contains the sensor's internal noise and human-generated features such as the respiration patterns as noise, which, fortunately, can mostly be removed during the filtering phase. We will show, in Section 6, how *HeartQuake* performs when the geophone is placed at different mattress locations, when using different mattress types, and also under various measurement conditions (e.g., different postures and motions).

Overall, the combined data (i.e., self-collected and CEBS data) used for model design and initial testing was gathered from 41 subjects (~1,400 minutes) containing both ECG and vibration data.

5.2 Deep Learning Model in *HeartQuake*

The deep learning model architecture in *HeartQuake* is designed using two-stacked Bi-LSTMs and three fully connected layers as illustrated in Figure 6. We use Bi-LSTMs model to ensure that the importance of the input sequence data is equally balanced among the early and late sequences. Simply using a basic LSTM could result in the earlier sequences of the data being treated less importantly than the later as the input passes through multiple cells in the network [36]. However, a Bi-LSTM performs one learning phase in one direction and another in the other direction of the input [88]. This allows the input sequences to equally impact the model when training.

Note that our model should map the non-linear relationships between various vibration signal inputs with the corresponding ECG signal as output. Thus, given that there are a large set of possible "next sequence" options in the vibration wave sequence, our model should be able to select its next step from a wide range of possible expressions. The work by LeCun et al. suggests that the use of a *stacked* Bi-LSTM architecture can be effective in such scenarios [55]. Based on these previous observations and our empirical evaluations, *HeartQuake* incorporates two sequentially stacked Bi-LSTMs.

The additional hidden layers and pipelines introduced by the stacked Bi-LSTM, when combined at a fully connected layer, are reunited to present the learned expressions from the previous layer in abstract form [34, 71]. By connecting three of these fully connected layers in serial, we achieve an effective pipeline for extracting the accurate ECG waveforms.

Finally, the inputs to our model in Figure 6 are vibration data with the size of 750 data points and the output is the same length of estimated ECG data (T=750). Since input vibration signals are sampled at 250 Hz, we concatenate three seconds of data to produce the model input. This is to ensure that all inputs contain at least two full heart beat "cycles" so that a relationship between two (or more) ECG peaks consists of a single input data sequence. This is important as some ECG-based clinical metrics, such as the RR interval, requires the time relationship between two consecutive ECG cycles. The input and output amplitude are normalized to the $[-1:1]$ range, and to account for this, we use the hyperbolic tangent (`tanh`) activation function for our Bi-LSTM model. All inputs of vibration/SCG and ECG are time synchronized in the training phase.

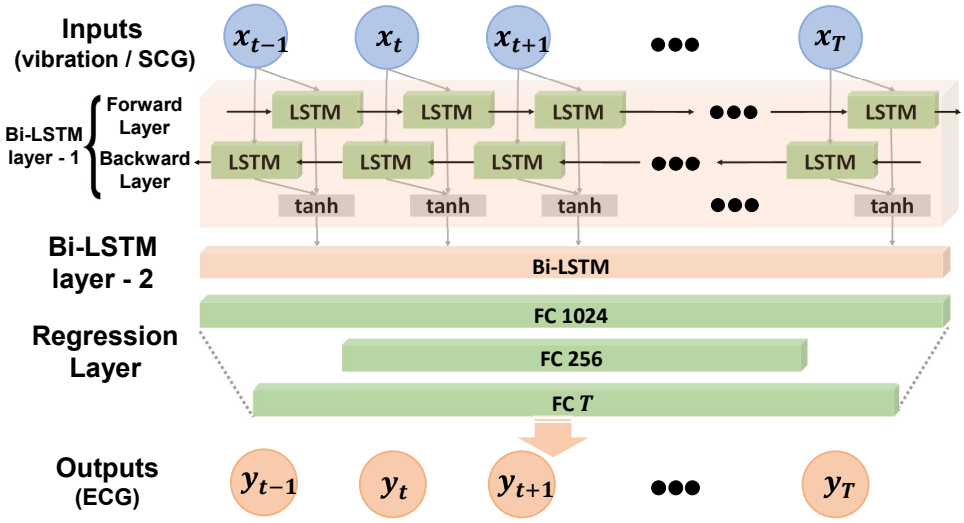

Fig. 6. *HeartQuake* ECG estimation model in *HeartQuake*

For model training, we use the data from the CEBS dataset to initially train the Bi-LSTM model. This allows the model to set the initial parameters, and we use a subset of our self-collected data (the training set) to perform fine-tuning on the parameters so that the model better fits our usage scenario.

6 EVALUATION

We now evaluate *HeartQuake* under different practical scenarios. As performance metrics, we chose (1) the error in estimated ECG peak timestamps compared to the ground truth, and (2) the percentage of detected ECG peaks. We selected these metrics given that, as we will later discuss, capturing the exact time of when each peak occurs is the basis of many clinical features that are extracted from the ECG signal (e.g., RR Interval, QRS segment width).

For accurately identifying peaks from both the estimated and ground-truth ECG signals, we use the widely adopted QRS detection algorithm proposed by Tompkins [69]. We point interested readers to [69] for detailed information on this scheme. From the detected Q, R, and S peaks, we also compute the highest value from the median RR interval of the subject to the Q-peak of the current ECG wave to identify the P-peak (the highest point of the P wave), and compute the highest value from the median from the S-peak to detect the T-peak (the highest point of the T wave). Note: all experiments were conducted on a foldable bed with a couch-type mattress unless explicitly specified.

6.1 Evaluation with the Baseline Dataset

We begin evaluating *HeartQuake* using the baseline data collected in Section 5.1. For training data, we used all of the data gathered from the CEBS dataset (procedure detailed in Section 5.2), and included two thirds of our self-collected baseline dataset (i.e., 14 out of 21 subjects) for model fine-tuning. Thus, we performed three-fold cross validation, in which we tested with different training and test data samples within the baseline dataset.

Table 2 presents *HeartQuake*'s peak detection rate, which is higher than 98% for all cases. The missing peaks were distributed (i.e., *HeartQuake* did not produce multiple continuous seconds of missing peaks).

Figure 7 presents the peak estimation accuracy of *HeartQuake*. Note that we only report values for the successfully identified peaks. Specifically, the R peak estimation showed the smallest error (~10 msec) among the five ECG peaks. Based on findings from the literature, this error is tolerable in computing various clinically useful

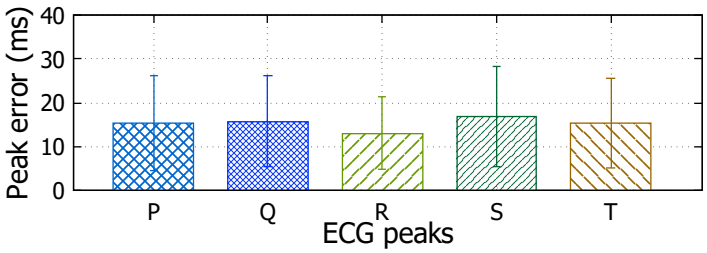

Fig. 7. Peak timestamp detection error.

Table 2. Peak detection rate for baseline data samples.

ECG peak	P	Q	R	S	T	Avg.
Detect rate (%)	99.81	98.46	99.66	99.05	99.45	99.29

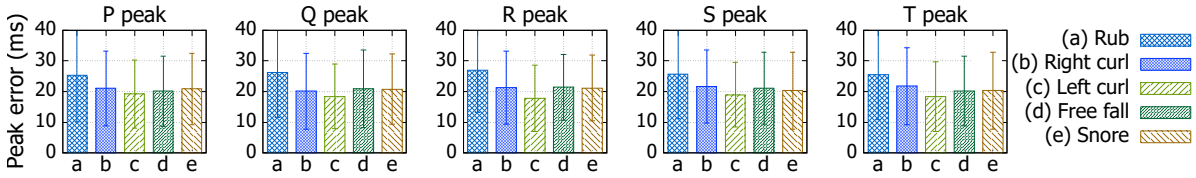

Fig. 8. Peak timestamp estimation error observed for different sleeping posture/activities.

features from the ECG such as heart rate variation [60, 93], which can assist in the early detection of cardiac disorders such as arrhythmia [79]. On the other hand, the estimation error of the P and Q peaks showed relatively higher errors (~17 msec) compared to the other peaks. We note that the P and Q peaks are known to show high variations with respect to the lead attachments even when using clinical-grade devices [3, 32]. Therefore, a higher peak detection error for P and Q is somewhat expected given that the ground truth measurements for these peaks (using the BioHarness) can be affected by small variations on how the device is worn.

Overall, the average estimation error over all peaks was 13.26 msec for this experiment. Given a person with a heart rate of 75 bpm, this error translates to only 1.10% on the time scale. Later in Section 7.1 we will evaluate the performance of *HeartQuake* from the perspective of various clinically used temporal features.

6.2 Impact of Motion and Posture

While the results above suggest that *HeartQuake* can accurately estimate the ECG peak timestamps, the data samples used for that experiment were collected under the assumption that users are stationary (i.e., no unnecessary movements) and always facing up on the bed. In reality, people can change between different postures and make spontaneous motions while sleeping and this could affect *HeartQuake* as these movements introduce additional varying noise and attenuation patterns to the vibrations generated at each heartbeat.

From video recordings of people's sleeping patterns (using videos gathered from a longitudinal dataset as we will discuss in Section 7.2), we were able to identify five different types of common motions and postures: (1) touching or rubbing the face or body with hands, (2) curled up sleeping to right, (3) curled up sleeping to left, (4) sleeping in a free-fall position - chest facing downwards, and (5) snoring. We designed a simple experiment to

Table 3. Detection rates for experiment with different sleeping postures/motions.

ECG peak		P	Q	R	S	T	Avg.
Detect rate (%)	Rub	99.27	97.74	98.82	98.82	98.83	98.92
	Right curl	99.89	98.85	99.89	99.89	98.89	99.48
	Left curl	97.83	98.75	99.95	98.75	98.21	98.70
	Free fall	99.90	98.82	99.72	99.72	98.35	99.30
	Snore	99.79	99.04	99.61	99.68	99.00	99.43

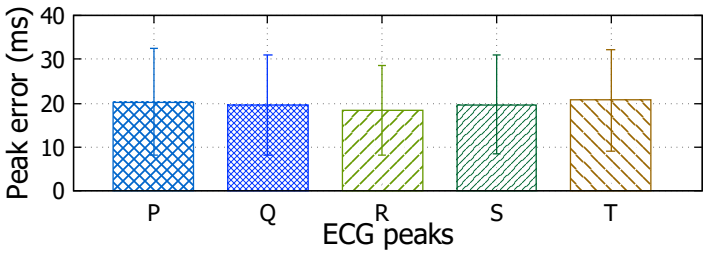

Fig. 9. Errors observed with external vibrations.

collect samples of these five different types of motions and postures from five participants that also took part in our baseline data collection. We ask the study participants to mimic the five different types of activities so that we have a controlled data set with these postures and gestures. Overall, we gathered 27 minutes of data for face/body rubbing, 80 for left curl, 80 minutes for right curled sleeping, 72 minutes for the free-fall posture, and 30 minutes of snoring data. Note that in these evaluations, we do not consider cases in which multiple postures and motions are performed simultaneously.

Figure 8 presents the ECG peak estimation accuracy for the five different postures/motions, and Table 3 presents the peak detection rate for each case. Over all cases, the average peak estimation error is 21.46 msec. It is interesting to note that the free-fall posture does not show the best performance despite having the heart being in close proximity to the mattress. This is because the geophone has a fixed location on the mattress, and flipping over in the free-fall posture lengthens the heart's distance to the sensor, which reduces the vibration amplitude and increases the error compared to the facing-up posture. Another interesting observation is that the left curl posture shows a lower error than right curl as the left curl posture places the heart is closer to the mattress.

To summarize, the inclusion of various motion artifacts by the bed occupant increases the estimation error. Especially for the face/body rubbing case, the error increases to up to ~28 msec. Fortunately, these motions, such as rubbing the face, do not typically occur persistently throughout the entire sleep cycle. Once the motion ends, our system can elevate back to a higher estimation accuracy. Furthermore, as we will show later in Section 7.1, typical ECG-related features used by doctors have error bounds that are larger than 40 to several hundreds of milliseconds; thus, such increased ECG peak estimation errors of *HeartQuake* can still be considered acceptable.

6.3 Impact of External Vibrations

While a user's surrounding environment is typically stable during the night, there can be cases where external noise, such as people moving around the bed, can affect the geophone measurements. We need to consider these cases as prior work has shown that geophones are sensitive enough to capture the vibrations generated by people

Table 4. Peak detection with external vibrations.

ECG peak	P	Q	R	S	T	Avg.
Detect rate (%)	99.90	98.46	99.83	97.37	97.88	98.69

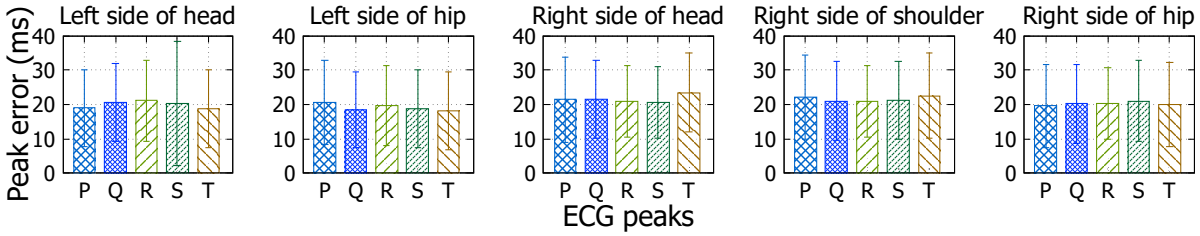

Fig. 10. Peak estimation error for measurements taken at different sensor installation locations.

Table 5. Peak detection rate for different sensor installation locations.

ECG peak		P	Q	R	S	T	Avg.
Detect rate (%)	**Left head**	98.66	97.99	99.35	97.39	99.30	98.54
	Left shoulder	99.81	98.46	99.66	99.05	99.45	99.29
	Left hip	97.96	99.70	99.60	99.52	98.80	99.12
	Right head	98.33	98.47	99.43	98.47	97.00	98.34
	Right shoulder	98.31	98.94	99.39	98.34	98.01	98.80
	Right hip	99.48	98.66	99.51	98.66	97.76	98.81

walking near it [64]. To observe the robustness of *HeartQuake* under externally generated vibrations, we designed a test in which we collected data similar to the baseline dataset, with no motions *on* the bed while facing up, but with one person walking continuously near the bed (within a 2-3 meter range). This experiment was carried out for five participants, each generating 10 minutes of data.

Figure 9 shows that compared to the case with no external vibrations, the peak estimation error increases only slightly, to 18-21 msec. In Table 4 we also see a small drop in the peak detection rate compared to stable environments – still 98.7% of the peaks are captured successfully.

6.4 Impact of Sensor Location

Next, we examine the impact of installing the geophone at different locations of the mattress. While all of our experiments until now placed the sensor at the left shoulder position of the mattress, we installed the sensor at five other locations: (1) right shoulder, (2) left hip, (3) right hip, (4) right head, and (5) left head, while the participants were facing up. Five participants took part in the measurements and for each location, geophone measurements were captured for 10 minutes per participant; totaling 50 minutes of data for each location.

Figure 10 plots the ECG peak estimation errors obtained for each sensor location and Table 5 presents the respective peak detection rates. Overall, the mean peak detection error measurements are similar to the case with different postures and show error values between 18-23 msec. Comparing these results with the case when the sensor was installed near the heart in Figure 7, suggests that locating the sensor closer to the origin of the

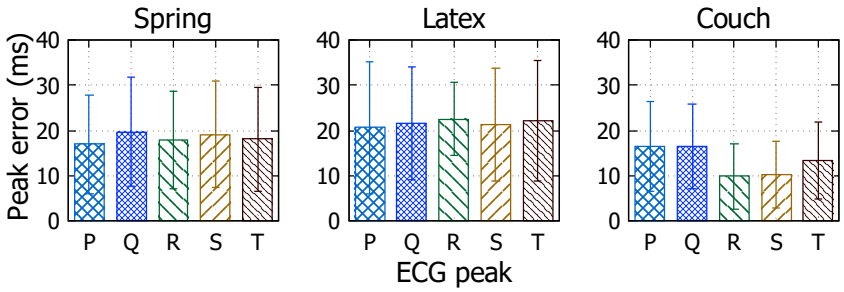

Fig. 11. Detection errors for different mattresses.

Table 6. Peak detection rate for different mattresses.

ECG peak		P	Q	R	S	T	Avg.
Detect rate (%)	**Spring**	99.68	98.80	99.11	98.81	99.35	99.15
	Latex	98.18	98.37	99.35	97.07	98.23	98.24
	Couch	99.81	98.46	99.66	99.05	99.45	99.29

heartbeat can help improve the accuracy but is not a crucial factor for operation. Nevertheless, this result still implies that *HeartQuake* will perform at its best if the bed occupant's sleep direction is predetermined. For general wards in the hospital (and for most at-home deployments), this will not be a strong assumption to make. Including additional geophone sensors on the bed can potentially help in identifying a vibration signal with the highest signal-to-noise ratio (SNR) to achieve low estimation errors.

6.5 Performance on Different Mattresses

Finally, we examine how *HeartQuake* performs with different bed types. In addition to the couch-type foldable bed used until now, we collected data from both a university hospital's general ward bed consisting of a latex mattress and a typical home-use spring mattress. In all cases, the geophone was attached to the mattress' top panel at the left shoulder position. We collected 30 minutes of data for each mattress type from three participants.

The results in Figure 11 presents the peak estimation error on the three bed types and Table 6 presents the detection rates. Compared to a couch-type mattress, the results for the spring-type and latex-type beds show an increase in peak prediction error (average 18.34 msec for spring-type and 21.61 msec for latex compared to 13.26 msec for couch type). The peak detection ratios for each mattress type also show similar patterns. We believe this is due to our model training being done with data collected from a couch-type mattress. Thus, the accuracy for patterns captured on other bed types dropped, and we conjecture that adding more diverse training data on a per-mattress basis can mitigate this error.

6.6 General vs. Personalized Models

The experiments up to now were for a general model, where previously collected samples of a participant included in the test set were not at all used for training purposes. We selected to do so because the goal of *HeartQuake* is to design a globally-applicable system. Now we see how *HeartQuake* works when the model is personalized.

Using our two motivating scenarios as a guide (Section 2.2), when used in general wards, additional personalized training data for target patients, can be obtained from the physiological signal ground-truth measurements

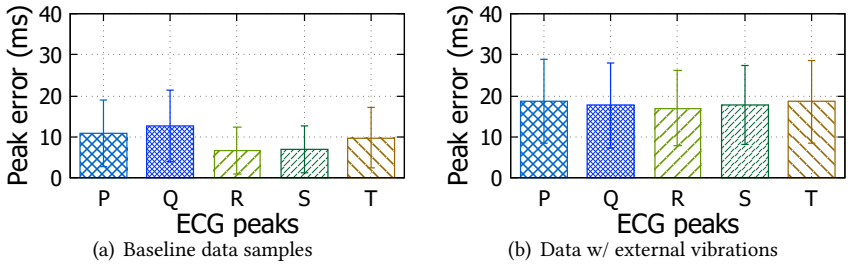

(a) Baseline data samples (b) Data w/ external vibrations

Fig. 12. Peak detection errors with and without external vibrations when using the *personalized* model.

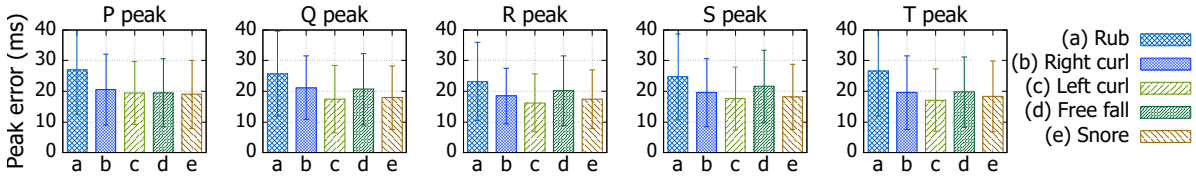

Fig. 13. Peak estimation error observed with *personalized model* for different postures and motions.

captured by the nursing staff during periodic rounds. Furthermore, when used at home, wearable ECG monitors can be used to bootstrap *HeartQuake* with personalized measurements as well.

With this motivation, we train a "personalized model" that, in addition to using the original training set, also includes a subset of data from all subjects from our baseline data collection (Sec. 5.1) for training. We leave out 20% (12 minutes) of data from each participant for testing. We also used data from the five participants that took part in the experiments discussed in Sections 6.2 (motions and postures) and 6.3 (external vibration) as testing data as well. These participants also took part in the baseline data collection phase; thus, we included their initially collected data (i.e., data with no motions while facing up) for training the personalized model and used the other data for testing only.

Figure 12(a) shows the peak estimation accuracy for the baseline data set (i.e., no motion; facing up) using the personalized model. Compared to results in Figure 7, the error is noticeably lower for all peaks. Specifically, the R peak error decreased from 9.83 msec to 6.66 msec. Overall, the average estimation error across all five peaks dropped from 13.26 to 9.37 msec with an average peak detection rate of 99.64%. Figure 12(b) plots the peak estimation errors for the dataset with external vibrations. Compared to Figure 9, we see a 9.17% decrease in average estimation error from 19.71 to 17.90 msec. with 99.30% average peak detection rate. Furthermore, when comparing the results for the personalized model using data collected for different motions and postures in Figure 13 with the results from the general model in Figure 8, we observe that the original error of 19-28 msec is reduced to 16-26 msec. For this data set, the average peak detection rate for all five peaks was 99.20%.

This suggests that using a personalized model can improve *HeartQuake*'s peak detection performance and as we show later in Section 7.2 adding more personalized data can further improve the peak estimation performance.

6.7 Amplitude

Our results show that *HeartQuake* can make accurate estimations on the timestamp at which each of the five core ECG peaks occur. However, to accurately estimate the final ECG waveform, we also need to confirm that the proper amplitude for each peak is well-estimated. Clinically, peak time-based metrics convey a comprehensive set

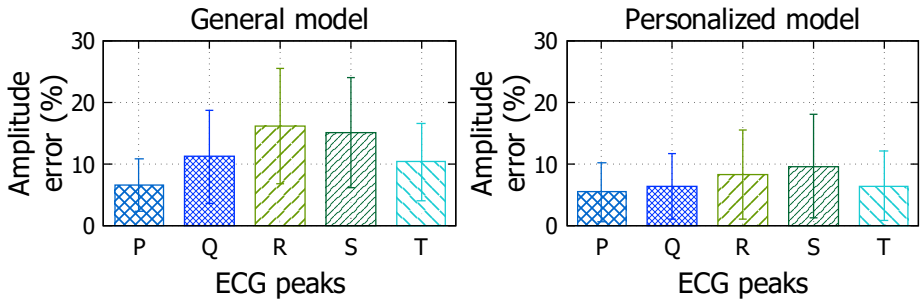

Fig. 14. Normalized estimation errors for each ECG peak's amplitude for baseline dataset.

of information, but the amplitude of the signal is also considered important for diagnosing some types of disorders (e.g., subendocardial ischemia [75], myocardial ischemia [26], etc.) and also in visualizing the morphology of an ECG signal.

In Figure 14 we show the error in the observed amplitude for each peak using the baseline dataset for both the general and personalized models. Given that we normalize the output ECG to the range of $[-1:1]$, the errors we observe in Figure 14 can be considered to be very low. On average, the absolute peak amplitude estimation error is 0.11 and 0.07 compared to the ground truth for the general and personalized models, respectively. This translates to 11.89% and 7.23% error compared to the ground truth. According to a report published by the American National Standards Institute, for routine visual ECG readings, the tolerated error for ECG amplitude is 10% or less [51]. While the generalized model is insufficient to meet this tight requirement, the results suggest that with a small amount of personal ECG data training, accurate amplitude estimation using *HeartQuake* is possible.

7 USING *HEARTQUAKE* FOR CLINICAL AND DAILY USE

As shown in the previous section, *HeartQuake* shows good performance in various situations and configurations. However, the next question is how the system fares when used in clinical environments and when used daily over a full sleep cycle. Validating this is especially important since these results can suggest the overall (potential) usability of *HeartQuake* in real-world applications.

7.1 *HeartQuake* as a Clinical Tool

7.1.1 What Do the Numbers Say?: The main goal of *HeartQuake* is to estimate the ECG waveform and its peaks' occurrence times as accurately as possible. Nevertheless, when clinical doctors observe the ECG, they look for specific features that are computed from the signals. Heart rate is one of such features in which the average number of R peaks is counted over a minute. As we mentioned earlier, a number of different factors, such as the RR interval, QRS complex width, ST segment length, QT interval, PR segment length, and PR interval, are needed to identify abnormal cardiovascular conditions such as various types of arrhythmia and heart block (c.f., Table 1). Figure 15 presents how these metrics can be computed using the ECG waveforms. We also show the typical range used to determine the normal conditions of each feature.

In Figure 16, we show how *HeartQuake* estimates the five clinical metrics of our interest. Notice that for all cases, the estimation error is lower than 30 msec. Especially for the RR interval when using the personalized model, the error from the ground truth is <3 msec. This suggests that we can make very accurate measurements on metrics that use intervals between multiple ECG R peaks. The error that we see in Figure 16 and throughout the evaluations suggest that *HeartQuake* provides accurate enough samples to be used as references for clinical purposes. We note that the standard grid used when plotting the ECG is represented by 0.04 sec columns [109]

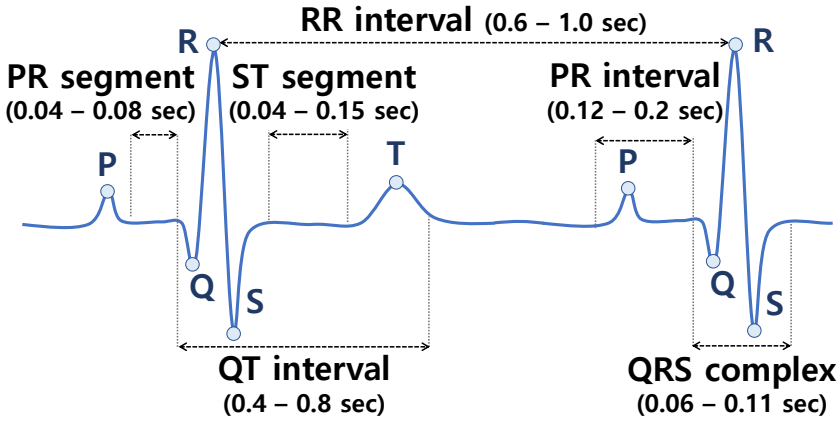

Fig. 15. Clinical features used in an ECG waveform with typical expectation ranges for normal condition diagnosis [21, 32, 104, 108, 109].

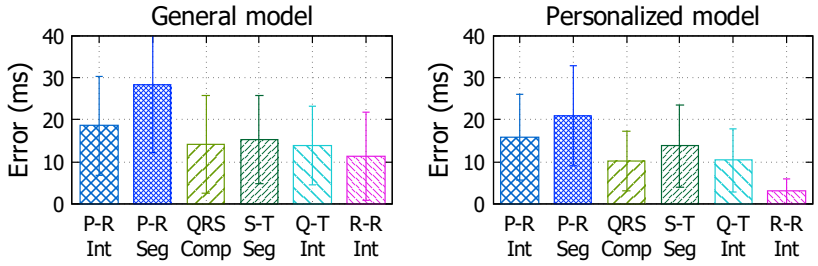

Fig. 16. Estimation errors for ECG-based features.

and the range of determining abnormal patterns in the ECG is defined over timescales between 40 to multiple hundreds of milliseconds [25, 84, 109].

7.1.2 What Do the Doctors Say?: Next, we took the body-attached sensor-collected and *HeartQuake*-generated ECG data from five random subjects in our self-collected baseline and CEBS dataset, and conducted a qualitative study with 11 clinical doctors practicing at six different university hospitals. Specifically, four cardiologists (one assistant professor and three associate professors), three infectious disease physicians (two associate professors and one full professor), two emergency medicine physicians (both assistant professors), and two traumatologists (both full professors in which one is the department chair) with an average of 10.8 years of practice (stdev 7.26) participated in our study. We presented the doctors with a total of 10 ECG patterns (10 seconds of data each; five ECG waveforms from body-attached sensors and the corresponding *HeartQuake*-generated ECG waveform pair) while not disclosing how the waveforms were paired. We randomly displayed the 10 ECG patterns to the study participants to remove bias. Among the five pairs of ECG waveform samples, we selected two pairs (four samples) that contain irregular heartbeats and one pair (two samples) with preliminary signs of ST-elevation. We select such samples given that, irregular heartbeats are detected using precise peak occurrence times, and ST-elevation requires accurate signal amplitude information to correctly diagnose. Note that these abnormal samples were from the CEBS dataset (with *HeartQuake* generating ECG based on the corresponding SCG data) as

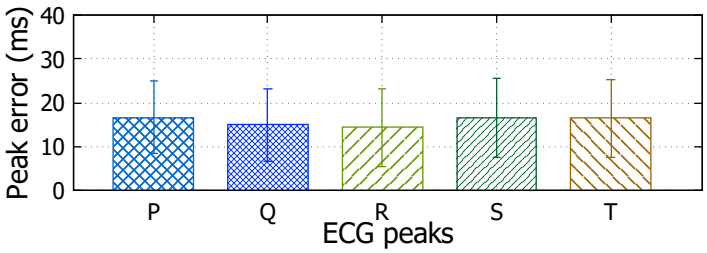

Fig. 17. Peak detection errors for longitudinal study with general model.

all our test subjects in the self-collected dataset were healthy. The other two pairs of ECG patterns were from patients with no known-cardiac disorders. Specifically, among the 10 samples, ECG samples #1, #4, #7 and #10 showed irregular heartbeat patterns (where [#1,#4] and [#7,#10] were "pairs") and samples #3 and #6 were a pair from a subject with mild ST-elevation. After presenting this data, we ask the study participating physicians the following three questions.

(1) Please identify any clinical anomalies from the 10 ECG signals.
(2) The 10 ECG waveforms were collected from 5 participants, one waveform is from a medical-grade ECG and the other is generated from *HeartQuake* based on the bed vibrations for the same time frame. Please group the 10 waveforms into 5 sets – where each set contains the waveforms for a specific participant. Note: we did not tell the doctors which waveforms were authentic and which were synthetically generated from *HeartQuake*.
(3) Please try to identify which of the 10 waveforms are generated from *HeartQuake* and which are authentic ECG signals. Briefly discuss why.

For question (1), we noticed that all 11 study participants successfully identified the four samples with irregular heartbeat patterns, and 7 of the 11 participants (63.6%) noticed the ST-elevation in samples #3 and #6. This suggests that the output ECG signal that *HeartQuake* produces has a good quality for clinical use and certainly can serve as an effective screening tool for further analysis.

Furthermore, all study participants correctly mapped the ECG pairs collected from body-attached sensors and *HeartQuake* (question (2)). This indicates that the similarity of ECG waveforms generated by *HeartQuake* compared to medical grade body-attached sensors is high and clinical professionals can easily recognize that the two waveforms are the same samples.

The responses for question (3) were interesting. All but one study participant failed in accurately guessing which of the samples were *HeartQuake*-generated and which were not. In fact, 5 of the 11 participants noted that they were not confident in distinguishing between the two types of signals. For the participants with valid responses (i.e., that actually made a "guess", either right or wrong), the average score of accurate guesses was only 2.7 out of 5. This again suggests that the two types of signals are indistinguishable, even for experienced specialists. This result along with the results from questions (1) and (2) comprehensively suggest that the quality of ECG patterns that *HeartQuake* generates is accurate enough to make clinical diagnosis (at least good enough as a screening tool) and they are not easily distinguishable from ECG signals collected from medical-grade body-attached sensors.

7.2 Longitudinal Study

While the baseline dataset (and all other data used in Section 6) was collected for short durations, we now examine the performance of *HeartQuake* in a more longer term "in-the-wild" setting via a longitudinal study. In this study,

Table 7. Detection rates for different sleeping activities.

Posture	Frequency	Avg Error (msec)	stdev	Posture	Frequency	Avg Error (msec)	stdev
Lying (face up) Still	63.84%	15.83	8.63	**Rubbing**	0.89%	25.01	14.66
Right Curl	16.65%	21.12	11.54	**Left Curl**	10.79%	18.73	10.05
Free Fall	1.12%	19.94	11.10	**Snoring**	6.71%	26.81	16.18

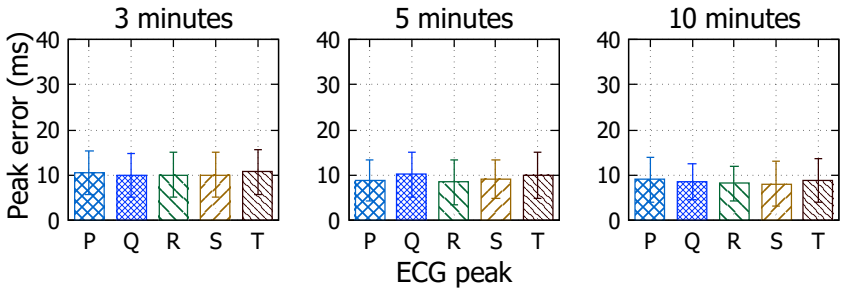

Fig. 18. Peak detection errors for longitudinal study with personal model trained with different lengths of personal data.

we recruited 15 additional volunteers (different from the 21 from the baseline dataset; 12 male, 3 female; avg age: 27.5 stdev: 2.69) to collect data for longer durations while the participants were sleeping. Specifically, we configure a room environment with a couch-type bed in which the study participants can sleep and collect both the geophone sensing (vibration) data and Bioharness 3-based ECG signals. Furthermore, to accurately identify and label different motions during their sleep we video recorded their sleep. For the longitudinal study dataset, we gathered a total of 71.7 hours of sleep activity (per participant average 4.77 hrs of sleep with stdev 1.72).

In Figure 17 we present the peak estimation errors for the longitudinal study dataset when applying a general (non-personalized) model used in Section 6.6. We did not perform any addition training with the newly collected data and used the entire dataset as test data only. Compared to the results in Figure 7, we can see that the average peak estimation error increases for most peaks (16.46 to 16.66 msec for P, 9.83 to 14.42 msec for R, 10.26 to 16.63 msec for S, and 13.30 to 16.50 msec msec for T peaks), but only slightly, which should not affect any application-level decision-making. For the Q-peak we actually see a decrease in error (from 16.42 to 14.94 msec), but the difference with the baseline dataset is yet marginal. The overall slight increase in error can be explained by the fact that when collecting the longitudinal dataset, we set no restrictions on participants' motions when on the bed. Thus, the dataset includes a mixture between different motions and idle postures. In Table 7 we present the accuracy of *HeartQuake* with respect to different postures. The labeling of each motion was done manually based on the video recordings of each participant's sleep. Participants were facing up and lying still for 63.8% of the entire period, and for these samples, the average accuracy of peak estimation is 15.83 msec. The next most frequent posture was the right curl posture (16.7%) with an average peak estimation accuracy of 21.12 msec. Together, the results reported in Figure 17 and Table 7 suggest that the results from the longitudinal study agree with the results for the baseline dataset.

Next, we examine the impact of using a personalized model on the longitudinal dataset. Specifically, we fine-tune the previously used general model with idle state data from each of the study participants. Specifically, we train three models for each participant in which 3, 5 and 10 minutes of personal data was used for model training (personalization), respectively. In Figure 18 we plot the average peak estimation error for each of the five ECG peaks with varying training data lengths. We can make two main observations from these plots. First, by

comparing with Figure 17 we can notice that, in-line with the results in Section 6.6, the use of a personalized model can help improve the overall peak estimation performance. Quantitatively, compared to the general model results in Figure 17, the overall average peak estimation latency is 10.13 msec when only 3 minutes of data is used for model personalization compared to 15.83 msec when applying the general model. Second, another interesting observation we can make when comparing the plots for the three different lengths of personal data used for training, is that even a small amount of personal data (3 minutes) can help improve the peak estimation performance, while adding more data for model personalization can effectively reduce the peak estimation performance.

7.3 Summary of Results and Next Steps

Overall, our evaluations in Sections 6 and 7 show the effectiveness of using *HeartQuake* as a useful screening tool for patient care. We were unable to report any results from real patients due to IRB and medical board privacy and safety reasons. However, our tests indicate that *HeartQuake* will be effective at detecting a range of heart-related conditions accurately, cheaply, and in a non-intrusive way. We are currently in the process of deploying *HeartQuake* at the cardiology ward of a hospital for real field trial and also have interest from the oncology ward of another hospital for a different pilot deployment study.

8 DISCUSSION

We have shown *HeartQuake* enables non-invasive ECG sensing using vibrations collected from a bed. The system is still evolving and we now discuss limitations and future work.

- **Estimation accuracy under seizures:** In extreme situations where the bed's occupants experience severe seizures and violent motions (e.g., heart attack), their posture can continuously change and the assumption of having the body on the bed surface may not hold. In these situations, the current design of *HeartQuake* may fail in providing clear ECG signals. Fortunately, the geophone installed under the bed can identify the unexpected motions and we plan to add a seizure detection model to *HeartQuake* to provide a comprehensive emergency alert system for clinical staff.
- **Distinguishing ECGs for multiple bed occupants:** When a single bed is shared by multiple people, *HeartQuake* will capture more than one heart-generated vibration pattern. Previous work by Jia et al. [47] show promising potential indicating that distinguishing the heartbeat of more than one person is possible using bed-attached geophones when using *multiple* geophones. As part of future work and deeper practicality testing, we plan to apply similar techniques (e.g., amplitude modulation, spatial information extraction) to separate multiple signals and capture the ECG for more than one bed occupant.
- **Cost benefits:** A key consideration of this research was to build a cost effective solution. As described earlier, accurate monitors used in hospitals exceed $10,000 [72], and commercial Holter monitors cost $2,000 [1] to $4,000 [63] per device. Wearable devices are cheaper ($400 [76] to $600 [2], but they are still cumbersome to wear during sleep. Our solution costs about $100 in parts ($60 for the Geophone sensor [96], $30 for the Raspberry Pi 3 [95], and $10 for misc. connectors). We expect the final cost of each device to be at most $200 to $300 after factoring in further development, economies of scale, integration, testing, and certification costs for commercialization. This is still an order of magnitude cheaper than existing solutions.
- **Performance on different surfaces:** While our evaluations show that the performance of *HeartQuake* can hold for three different types of mattresses, due to practical limitations, we were not able to test the performance on additional mattress form-factors. For example, memory foam or water mattresses will show different vibration propagation patterns compared to the ones we tested in Section 6.5. While we were not able to empirically validate *HeartQuake*'s effectiveness in such environments, we conjecture that the change of mattress types will mostly impact the input signal amplitude, given that the frequency characteristics of the

heart beats and noise patterns will mostly stay the same. There may, however, be changes to the hardware configurations (e.g., sensor installation location, amplifier parameters) to adjust for the new environments. In any case, we see this as an essential part of our future work prior to commercially applying *HeartQuake* to diverse practical environments.

- **Case-study – Arrhythmia Detection:** The samples used for our evaluation were collected from participants with no reported cardiac disorders. This was because collecting samples from real patients with heart problems (asking them to be on our beds) was not possible through our study due to IRB and medical board safety reasons. However, it is important that the system is also tested and validated for subject with abnormal cardiac conditions prior to the large scale deployment in real-world settings. While not in scale, fortunately, we noticed that patient record `m004` of the CEBS dataset was collected from a patient with ectopic heart beats (premature ventricular contraction). We use this data, which consists of 3,000 seconds of ECG and SCG data with 57 abnormal heartbeats, as input for *HeartQuake* to observe the capability of *HeartQuake* in identifying abnormal cardiac conditions. Specifically, for this mini-test, we re-trained our model *without* using any data from patient `m004` and tested the accuracy of our Bi-LSTM-based ECG estimation model. Patient `m004`'s SCG data was used as input and *HeartQuake* generated the corresponding ECG signals, and we compare this with the ground truth ECG from the CEBS dataset. We note that 97.4% of ECG peaks were successfully captured using *HeartQuake* and the average peak estimation error for five peaks was 16.4 msec (14.6 for P, 21.01 for Q, 15.80 for R, 12.11 for S, and 18.65 msec for T). While more studies are essential, out mini-test result with `m004`'s data can be a preliminary indicator suggesting that *HeartQuake* can detect abnormal ECG patterns.

9 RELATED WORK

Recent development in various sensing technologies has enabled a number of novel systems for non-intrusive cardiac activity monitoring. Zhao et al. presented a system for detecting heart beats and respiration by combining deep learning models with features extracted from RF signals in a smart home environment [116]. In addition to RF, there have also been efforts to implement heart rate monitoring systems with images or videos of target subjects [40, 74, 93, 101].

Dinh et al. [30] and Siecinski et al. [92] proposed schemes to collect SCG data using a smartphone accelerometer for capturing cardiac activity features. Similarly, Chao et al. [20] designed a small multi-sensor platform on a flexible board for wireless tri-axial SCG, single-lead ECG, and single-point skin temperature monitoring and Jain et al. [44] proposed a portable system that captures chest-attached SCG sensors for long-term SCG monitoring.

For systems using geophone sensors, Bonde et al. proposed a system using bed-installed geophones to capture the RR interval from bed occupants [12] and Jia et al. presented a system to distinguish heartbeats of multiple users on a bed [47]. These works effectively show the feasibility of exploiting heart-generated vibrations for cardiac activity monitoring using abstract-level metrics.

These previously proposed schemes successfully capture a heart's cardiac rhythms in abstract form (i.e., heart rate or heart rate variability) and show feasibility in applying non-intrusive sensing to continuous heart monitoring applications. Essentially, our work shares similar goals in the fact that *HeartQuake* also enables cardiac monitoring in previously difficult situations, but **our work focuses on capturing accurate ECG waveforms** from non-intrusive sensing components, which is a much more complex task than simply measuring abstract features such as the heart rate.

10 CONCLUSION

We present *HeartQuake*, a low-cost, accurate, non-intrusive system for capturing ECG signals of a person lying on a bed. *HeartQuake* collects the vibration signals generated by the beating of the occupant's heart and uses a filter to eliminate noise introduced in the signal collection process. The filtered vibration signal is used as an input to a

Bi-LSTM-based deep learning model to generate corresponding ECG signals. We evaluate the ECG estimation performance of *HeartQuake* under various bed and user configurations using two different self-collected datasets and show that the accuracy of peak estimation is good enough to capture various clinically used ECG-related metrics. Furthermore, a qualitative study with 11 physicians suggests that *HeartQuake* generates ECG signals that are suitable for diagnosing abnormal cardiovascular conditions, and are difficult to distinguish from ECG waveforms collected from medical-grade ECG devices.

ACKNOWLEDGMENTS

This work was supported by the National Research Foundation of Korea (NRF) Grant funded by the Korean Government (MSIP) (No.2015R1A5A1037668).

REFERENCES

[1] 2019. SEER 1000 Holter Recorder. (2019). https://www.gehealthcare.com/products/diagnostic-ecg/ambulatory/seer-1000 Accessed on 06.08.2019.
[2] 2019. Zephyr BioHarness 3.0 User Manual. (2019). https://www.zephyranywhere.com/media/download/bioharness3-user-manual.pdf Accessed on 11.04.2019.
[3] Accessed on Dec.06 2019. The ECG leads: electrodes, limb leads, chest (precordial) leads, 12-Lead ECG (EKG). (Accessed on Dec.06 2019). https://ecgwaves.com/topic/ekg-ecg-leads-electrodes-systems-limb-chest-precordial/
[4] G.I. Alaminiokuma and W.N. Ofuyah. 2017. Performance of seismic detectors: a case study of the sensitivity of SM-4 geophones used in Nigeria. *International Research Journal of Earth Sciences* 5, 8 (2017), 32–40.
[5] Donald G Albert. 1987. The effect of snow on vehicle-generated seismic signatures. *The Journal of the Acoustical Society of America* 81, 4 (1987), 881–887.
[6] Donald G Albert, Shahram Taherzadeh, Keith Attenborough, Patrice Boulanger, and Stephen N Decato. 2013. Ground vibrations produced by surface and near-surface explosions. *Applied Acoustics* 74, 11 (2013), 1279–1296.
[7] John Allen. 2007. Photoplethysmography and its application in clinical physiological measurement. *Physiological measurement* 28, 3 (2007), R1.
[8] arrhy Accessed on 02.03.2019. Arrhythmia. (Accessed on 02.03.2019). https://www.heart.org/en/health-topics/arrhythmia
[9] Emelia J Benjamin, Paul Muntner, and Márcio Sommer Bittencourt. 2019. Heart disease and stroke statistics-2019 update: a report from the American Heart Association. *Circulation* 139, 10 (2019), e56–e528.
[10] R Bertolami, H Bunke, S Fernandez, A Graves, M Liwicki, and J Schmidhuber. 2009. A novel connectionist system for improved unconstrained handwriting recognition. *IEEE Transactions on Pattern Analysis and Machine Intelligence* 31, 5 (2009).
[11] Dwaipayan Biswas, Luke Everson, Muqing Liu, Madhuri Panwar, Bram-Ernst Verhoef, Shrishail Patki, Chris H Kim, Amit Acharyya, Chris Van Hoof, Mario Konijnenburg, and others. 2019. CorNET: Deep learning framework for PPG-based heart rate estimation and biometric identification in ambulant environment. *IEEE transactions on biomedical circuits and systems* 13, 2 (2019), 282–291.
[12] Amelie Bonde, Shijia Pan, Zhenhua Jia, Yanyong Zhang, Hae Young Noh, and Pei Zhang. 2018. VVRRM: Vehicular Vibration-Based Heart RR-Interval Monitoring System. In *Proceedings of the 19th International Workshop on Mobile Computing Systems and Applications (HotMobile '18)*. ACM, New York, NY, USA, 37–42. DOI: https://doi.org/10.1145/3177102.3177110
[13] Luigi Casacanditella, Gloria Cosoli, Sara Casaccia, Enrico Primo Tomasini, and Lorenzo Scalise. 2016. Indirect measurement of the carotid arterial pressure from vibrocardiographic signal: Calibration of the waveform and comparison with photoplethysmographic signal. In *2016 38th Annual International Conference of the IEEE Engineering in Medicine and Biology Society (EMBC)*. IEEE, 3568–3571.
[14] Paolo Castiglioni, Andrea Faini, Gianfranco Parati, and Marco Di Rienzo. 2007. Wearable seismocardiography. In *2007 29th Annual International Conference of the IEEE Engineering in Medicine and Biology Society*. IEEE, 3954–3957.
[15] CEBS Accessed on 02.03.2019. PhysioBank ATM. (Accessed on 02.03.2019). https://physionet.org/pn6/cebsdb/
[16] Centers for Disease Control and Prevention 2016. Open Data | Centers for Disease Control and Prevention | Chronic Disease and Health Promotion Data & Indicators. (2016). https://chronicdata.cdc.gov/ Accessed on 29.02.2019.
[17] Centers for Disease Control and Prevention 2017. National Center for Health Statistics. (May 2017). https://www.cdc.gov/nchs/fastats/deaths.htm Accessed on 29.02.2019.
[18] Nicolas Chin-Yee, Gianni D'Egidio, Kednapa Thavorn, Daren Heyland, and Kwadwo Kyeremanteng. 2017. Cost analysis of the very elderly admitted to intensive care units. *Critical Care* 21, 1 (2017), 109.
[19] Amer Abdulmahdi Chlaihawi, Binu Baby Narakathu, Sepehr Emamian, Bradley J Bazuin, and Massood Z Atashbar. 2018. Development of printed and flexible dry ECG electrodes. *Sensing and bio-sensing research* 20 (2018), 9–15.

[20] Yindar Chuo, Marcin Marzencki, Benny Hung, Camille Jaggernauth, Kouhyar Tavakolian, Philip Lin, and Bozena Kaminska. 2010. Mechanically flexible wireless multisensor platform for human physical activity and vitals monitoring. *IEEE transactions on biomedical circuits and systems* 4, 5 (2010), 281–294.
[21] Vivian L Clark and James A Kruse. 1990. Clinical methods: the history, physical, and laboratory examinations. *Jama* 264, 21 (1990), 2808–2809.
[22] J Cleland, H Dargie, S Hardman, T McDonagh, and P Mitchell. Accessed on Dec.10 2019. National Heart Failure Audit: April 2012-March 2012. London: National Institute for Cardiovascular Outcomes Research; 2013. (Accessed on Dec.10 2019). http://www.wales.nhs.uk/sitesplus/documents/862/National%20Heart%20Failure%20Audit%20April%202012-March2013.pdf
[23] David Conen, Martin Adam, Frederic Roche, Jean-Claude Barthelemy, Denise Felber Dietrich, Medea Imboden, Nino Künzli, Arnold von Eckardstein, Stephan Regenass, Thorsten Hornemann, and others. 2012. Premature atrial contractions in the general population: frequency and risk factors. *Circulation* 126, 19 (2012), 2302–2308.
[24] G Cosoli, L Casacanditella, EP Tomasini, and L Scalise. 2017. Heart Rate assessment by means of a novel approach applied to signals of different nature. In *Journal of Physics: Conference Series*, Vol. 778. IOP Publishing, 012001.
[25] John M. Costello, Mark E. Alexander, Karla M. Greco, Antonio R. Perez-Atayde, and Peter C. Laussen. 2009. Lyme Carditis in Children: Presentation, Predictive Factors, and Clinical Course. *Pediatrics* 123, 5 (2009), e835–e841. DOI: https://doi.org/10.1542/peds.2008-3058 arXiv:https://pediatrics.aappublications.org/content/123/5/e835.full.pdf
[26] David C Crossman. 2004. The pathophysiology of myocardial ischaemia. *Heart* 90, 5 (2004), 576–580.
[27] B. Barkat D. Boutana, M. Benidir. 2011. Segmentation and identification of some pathological phonocardiogram signals using time-frequency analysis. *IET Signal Processing* 5 (September 2011), 527–537(10). Issue 6. https://digital-library.theiet.org/content/journals/10.1049/iet-spr.2010.0013
[28] Marco Di Rienzo, Prospero Lombardi, Diana Scurati, and Emanuele Vaini. 2016. A new technological platform for the multisite assessment of 3D seismocardiogram and pulse transit time in cardiac patients. In *2016 Computing in Cardiology Conference (CinC)*. IEEE, 781–784.
[29] DigiTek XT 2019. Philips DigiTek XT. (2019). https://www.philips.com.au/healthcare/product/HC860322/digitrak-xt-holter-monitor Accessed on 07.08.2019.
[30] Anh Dinh. 2011. Heart activity monitoring on smartphone. In *International Conference on Biomedical Engineering and Technology*, Vol. 11. 45–49.
[31] Cheryl D Fryar, Te-Ching Chen, and Xianfen Li. 2012. *Prevalence of uncontrolled risk factors for cardiovascular disease: United States, 1999-2010.* Number 103. US Department of Health and Human Services, Centers for Disease Control and ....
[32] Tomas B Garcia. 2013. *12-lead ECG: The art of interpretation.* Jones & Bartlett Publishers.
[33] Felix A Gers, Nicol N Schraudolph, and Jürgen Schmidhuber. 2002. Learning precise timing with LSTM recurrent networks. *Journal of machine learning research* 3, Aug (2002), 115–143.
[34] Michiel Hermans and Benjamin Schrauwen. 2013. Training and analysing deep recurrent neural networks. In *Advances in neural information processing systems*. 190–198.
[35] Sepp Hochreiter and Jürgen Schmidhuber. 1997. Long Short-Term Memory. *Neural Comput.* 9, 8 (Nov. 1997), 1735–1780. DOI: https://doi.org/10.1162/neco.1997.9.8.1735
[36] Sepp Hochreiter and Jürgen Schmidhuber. 1997. Long short-term memory. *Neural computation* 9, 8 (1997), 1735–1780.
[37] Michael S Hons. 2008. Seismic sensing: Comparison of geophones and accelerometers using laboratory and field data. (2008).
[38] Tero Hurnanen, Eero Lehtonen, Mojtaba Jafari Tadi, Tom Kuusela, Tuomas Kiviniemi, Antti Saraste, Tuija Vasankari, Juhani Airaksinen, Tero Koivisto, and Mikko Pänkäälä. 2016. Automated detection of atrial fibrillation based on time–frequency analysis of seismocardiograms. *IEEE journal of biomedical and health informatics* 21, 5 (2016), 1233–1241.
[39] Sinh Huynh, Rajesh Krishna Balan, JeongGil Ko, and Youngki Lee. 2019. VitaMon: measuring heart rate variability using smartphone front camera. In *Proceedings of the 17th Conference on Embedded Networked Sensor Systems*. 1–14.
[40] IEEE 2012. *Validation of heart rate extraction using video imaging on a built-in camera system of a smartphone.* IEEE.
[41] iHealth 2019. iHealth Official Site for Smart Blood Pressure Monitor,Glucose Meter,Scale & More. (2019). https://ihealthlabs.com/ Accessed on 27.02.2019.
[42] Omer T Inan, Pierre-Francois Migeotte, Kwang-Suk Park, Mozziyar Etemadi, Kouhyar Tavakolian, Ramon Casanella, John Zanetti, Jens Tank, Irina Funtova, G Kim Prisk, and others. 2014. Ballistocardiography and seismocardiography: A review of recent advances. *IEEE journal of biomedical and health informatics* 19, 4 (2014), 1414–1427.
[43] Puneet Kumar Jain and Anil Kumar Tiwari. 2014. Heart monitoring systems-A review. *Computers in biology and medicine* 54 (2014), 1–13.
[44] Puneet Kumar Jain, Anil Kumar Tiwari, and Vijay S Chourasia. 2016. Performance analysis of seismocardiography for heart sound signal recording in noisy scenarios. *Journal of medical engineering & technology* 40, 3 (2016), 106–118.
[45] Michael Jerosch-Herold, John Zanetti, Hellmut Merkle, Liviu Poliac, Hong Huang, Abdoul Mansoor, Fan Zhao, and Norbert Wilke. 1999. The seismocardiogram as magnetic-field-compatible alternative to the electrocardiogram for cardiac stress monitoring. *The International Journal of Cardiac Imaging* 15, 6 (1999), 523–531.

[46] Zhenhua Jia, Musaab Alaziz, Xiang Chi, Richard E Howard, Yanyong Zhang, Pei Zhang, Wade Trappe, Anand Sivasubramaniam, and Ning An. 2016. HB-phone: a bed-mounted geophone-based heartbeat monitoring system. In *Proceedings of the 15th International Conference on Information Processing in Sensor Networks*. IEEE Press, 22.

[47] Zhenhua Jia, Amelie Bonde, Sugang Li, Chenren Xu, Jingxian Wang, Yanyong Zhang, Richard E. Howard, and Pei Zhang. 2017. Monitoring a Person's Heart Rate and Respiratory Rate on a Shared Bed Using Geophones. In *Proceedings of the 15th ACM Conference on Embedded Network Sensor Systems (SenSys '17)*. ACM, New York, NY, USA, Article 6, 14 pages. DOI: https://doi.org/10.1145/3131672.3131679

[48] Pedram Kazemian, Gavin Oudit, and Bodh I Jugdutt. 2012. Atrial fibrillation and heart failure in the elderly. *Heart failure reviews* 17, 4-5 (2012), 597–613.

[49] Farzad Khosrow-Khavar, Kouhyar Tavakolian, Andrew Blaber, and Carlo Menon. 2017. Automatic and robust delineation of the fiducial points of the seismocardiogram signal for noninvasive estimation of cardiac time intervals. *IEEE Transactions on Biomedical Engineering* 64, 8 (2017), 1701–1710.

[50] Shaan Khurshid, Seung Hoan Choi, Lu-Chen Weng, Elizabeth Y Wang, Ludovic Trinquart, Emelia J Benjamin, Patrick T Ellinor, and Steven A Lubitz. 2018. Frequency of cardiac rhythm abnormalities in a half million adults. *Circulation: Arrhythmia and Electrophysiology* 11, 7 (2018), e006273.

[51] Paul Kligfield, Leonard S. Gettes, James J. Bailey, Rory Childers, Barbara J. Deal, E. William Hancock, Gerard van Herpen, Jan A. Kors, Peter Macfarlane, David M. Mirvis, Olle Pahlm, Pentti Rautaharju, and Galen S. Wagner. 2007. Recommendations for the Standardization and Interpretation of the Electrocardiogram: Part I: The Electrocardiogram and Its Technology A Scientific Statement From the American Heart Association Electrocardiography and Arrhythmias Committee, Council on Clinical Cardiology; the American College of Cardiology Foundation; and the Heart Rhythm Society Endorsed by the International Society for Computerized Electrocardiology. *Journal of the American College of Cardiology* 49, 10 (2007), 1109 – 1127. DOI: https://doi.org/10.1016/j.jacc.2007.01.024

[52] J. Ko, C. Lu, M. B. Srivastava, J. A. Stankovic, A. Terzis, and M. Welsh. 2010. Wireless Sensor Networks for Healthcare. *Proc. IEEE* 98, 11 (Nov 2010), 1947–1960. DOI: https://doi.org/10.1109/JPROC.2010.2065210

[53] Mayank Kumar, Ashok Veeraraghavan, and Ashutosh Sabharwal. 2015. DistancePPG: Robust non-contact vital signs monitoring using a camera. *Biomedical optics express* 6, 5 (2015), 1565–1588.

[54] Sungjun Kwon, Hyunseok Kim, and Kwang Suk Park. 2012. Validation of heart rate extraction using video imaging on a built-in camera system of a smartphone. In *2012 Annual International Conference of the IEEE Engineering in Medicine and Biology Society*. IEEE, 2174–2177.

[55] Yann LeCun, Yoshua Bengio, and Geoffrey Hinton. 2015. Deep learning. *nature* 521, 7553 (2015), 436.

[56] Magdalena Lewandowska, Jacek Rumiński, Tomasz Kocejko, and Jędrzej Nowak. 2011. Measuring pulse rate with a webcam—a non-contact method for evaluating cardiac activity. In *2011 federated conference on computer science and information systems (FedCSIS)*. IEEE, 405–410.

[57] L.S. Lilly and H.M. School. 2011. *Pathophysiology of Heart Disease: A Collaborative Project of Medical Students and Faculty*. Wolters Kluwer/Lippincott Williams & Wilkins. https://books.google.co.kr/books?id=bIF7PckmFMoC

[58] Wen-Yen Lin, Wen-Cheng Chou, Po-Cheng Chang, Chung-Chuan Chou, Ming-Shien Wen, Ming-Yun Ho, Wen-Chen Lee, Ming-Jer Hsieh, Chung-Chih Lin, Tsai-Hsuan Tsai, and others. 2018. Identification of location specific feature points in a cardiac cycle using a novel seismocardiogram spectrum system. *IEEE journal of biomedical and health informatics* 22, 2 (2018), 442–449.

[59] Janet Lipski, Larry Cohen, Jaime Espinoza, Michael Motro, Simon Dack, and Ephraim Donoso. 1976. Value of Holter monitoring in assessing cardiac arrhythmias in symptomatic patients. *The American journal of cardiology* 37, 1 (1976), 102–107.

[60] S. Mahdiani, V. Jeyhani, M. Peltokangas, and A. Vehkaoja. 2015. Is 50 Hz high enough ECG sampling frequency for accurate HRV analysis?. In *2015 37th Annual International Conference of the IEEE Engineering in Medicine and Biology Society (EMBC)*. 5948–5951. DOI: https://doi.org/10.1109/EMBC.2015.7319746

[61] Sumit Majumder, Emad Aghayi, Moein Noferesti, Hamidreza Memarzadeh-Tehran, Tapas Mondal, Zhibo Pang, and M Deen. 2017. Smart homes for elderly healthcare - Recent advances and research challenges. *Sensors* 17, 11 (2017), 2496.

[62] David D McManus, Jane S Saczynski, Darleen Lessard, Menhel Kinno, Rahul Pidikiti, Nada Esa, Josephine Harrington, and Robert J Goldberg. 2013. Recent trends in the incidence, treatment, and prognosis of patients with heart failure and atrial fibrillation (the Worcester Heart Failure Study). *The American journal of cardiology* 111, 10 (2013), 1460–1465.

[63] Medtronic. 2019. Heart Monitors - Reveal LINQ ICM System. (2019). https://www.medtronic.com/us-en/patients/treatments-therapies/heart-monitors/our-monitors.html

[64] Mostafa Mirshekari, Shijia Pan, Jonathon Fagert, Eve M. Schooler, Pei Zhang, and Hae Young Noh. 2018. Occupant localization using footstep-induced structural vibration. *Mechanical Systems and Signal Processing* 112 (2018), 77 – 97. DOI: https://doi.org/10.1016/j.ymssp.2018.04.026

[65] MP36 Accessed on 02.03.2019. BIOPAC Systems, Inc. (Accessed on 02.03.2019). https://www.biopac.com/product-category/education/systems-education/

[66] Patrick Mullan, Christoph M Kanzler, Benedikt Lorch, Lea Schroeder, Ludwig Winkler, Larissa Laich, Frederik Riedel, Robert Richer, Christoph Luckner, Heike Leutheuser, and others. 2015. Unobtrusive heart rate estimation during physical exercise using photoplethysmographic and acceleration data. In *2015 37th Annual International Conference of the IEEE Engineering in Medicine and Biology Society (EMBC)*. IEEE, 6114–6117.

[67] Krzysztof Narkiewicz, Nicola Montano, Chiara Cogliati, Philippe JH Van De Borne, Mark E Dyken, and Virend K Somers. 1998. Altered cardiovascular variability in obstructive sleep apnea. *Circulation* 98, 11 (1998), 1071–1077.

[68] James Nolan, Phillip D Batin, Richard Andrews, Steven J Lindsay, Paul Brooksby, Michael Mullen, Wazir Baig, Andrew D Flapan, Alan Cowley, Robin J Prescott, and others. 1998. Prospective study of heart rate variability and mortality in chronic heart failure: results of the United Kingdom heart failure evaluation and assessment of risk trial (UK-heart). *Circulation* 98, 15 (1998), 1510–1516.

[69] Jiapu Pan and Willis J Tompkins. 1985. A real-time QRS detection algorithm. *IEEE Trans. Biomed. Eng* 32, 3 (1985), 230–236.

[70] Shijia Pan, Amelie Bonde, Jie Jing, Lin Zhang, Pei Zhang, and Hae Young Noh. 2014. Boes: building occupancy estimation system using sparse ambient vibration monitoring. In *Sensors and Smart Structures Technologies for Civil, Mechanical, and Aerospace Systems 2014*, Vol. 9061. International Society for Optics and Photonics, 90611O.

[71] Razvan Pascanu, Caglar Gulcehre, Kyunghyun Cho, and Yoshua Bengio. 2013. How to construct deep recurrent neural networks. *arXiv preprint arXiv:1312.6026* (2013).

[72] Philips N.V. 2019. IntelliVue MX 750 & 850 Bedside Patient Monitor. Available at: https://philipsproductcontent.blob.core.windows.net/assets/20190910/073a22d618ab4bd6a9afaac4013f2d19.pdf. (2019).

[73] Ming-Zher Poh, Daniel J McDuff, and Rosalind W Picard. 2010. Non-contact, automated cardiac pulse measurements using video imaging and blind source separation. *Optics express* 18, 10 (2010), 10762–10774.

[74] Ming-Zher Poh, Daniel J McDuff, and Rosalind W Picard. 2010. Non-contact, automated cardiac pulse measurements using video imaging and blind source separation. *Optics express* 18, 10 (2010), 10762–10774.

[75] Mark Potse, A-Robert LeBlanc, René Cardinal, and Alain Vinet. 2006. ST elevation or depression in subendocardial ischemia?. In *2006 International Conference of the IEEE Engineering in Medicine and Biology Society*. IEEE, 3899–3902.

[76] QardioCore 2019. Smart Wearable ECG EKG Monitor - QardioCore. (2019). http://www.getqardio.com/qardiocore-wearable-ecg-ekg-monitor-iphone/ Accessed on 28.02.2019.

[77] Ho-Kyeong Ra, Jungmo Ahn, Hee Jung Yoon, Dukyong Yoon, Sang Hyuk Son, and JeongGil Ko. 2017. I am a Smart watch, Smart Enough to Know the Accuracy of My Own Heart Rate Sensor. In *Proceedings of the 18th International Workshop on Mobile Computing Systems and Applications*. ACM, 49–54.

[78] Raspberry Pi Accessed on 29.02.2019. Raspberry Pi 3 Model B+. (Accessed on 29.02.2019). https://www.raspberrypi.org/products/raspberry-pi-3-model-b-plus/

[79] M.J. Reed, C.E. Robertson, and P.S. Addison. 2005. Heart rate variability measurements and the prediction of ventricular arrhythmias. *QJM: An International Journal of Medicine* 98, 2 (02 2005), 87–95. DOI:https://doi.org/10.1093/qjmed/hci018 arXiv:http://oup.prod.sis.lan/qjmed/article-pdf/98/2/87/4469061/hci018.pdf

[80] Anne B Riley and Warren J Manning. 2011. Atrial fibrillation: an epidemic in the elderly. *Expert review of cardiovascular therapy* 9, 8 (2011), 1081–1090.

[81] Jillian Riley. 2015. The key roles for the nurse in acute heart failure management. *Cardiac failure review* 1, 2 (2015), 123.

[82] Spencer Z Rosero, Valentina Kutyifa, Brian Olshansky, and Wojciech Zareba. 2013. Ambulatory ECG monitoring in atrial fibrillation management. *Progress in cardiovascular diseases* 56, 2 (2013), 143–152.

[83] Denis Roy, Mario Talajic, Stanley Nattel, D George Wyse, Paul Dorian, Kerry L Lee, Martial G Bourassa, J Malcolm O Arnold, Alfred E Buxton, A John Camm, and others. 2008. Rhythm control versus rate control for atrial fibrillation and heart failure. *New England Journal of Medicine* 358, 25 (2008), 2667–2677.

[84] Alex Sagie, Martin G. Larson, Robert J. Goldberg, James R. Bengtson, and Daniel Levy. 1992. An improved method for adjusting the QT interval for heart rate (the Framingham Heart Study). *The American Journal of Cardiology* 70, 7 (1992), 797 – 801. DOI: https://doi.org/10.1016/0002-9149(92)90562-D

[85] Prasan Sahoo, Hiren Thakkar, Wen-Yen Lin, Po-Cheng Chang, and Ming-Yih Lee. 2018. On the design of an efficient cardiac health monitoring system through combined analysis of ecg and scg signals. *Sensors* 18, 2 (2018), 379.

[86] Haşim Sak, Andrew Senior, and Françoise Beaufays. 2014. Long short-term memory recurrent neural network architectures for large scale acoustic modeling. In *Fifteenth annual conference of the international speech communication association*.

[87] Samsung Healthcare 2019. SamsungHealthcare Global. (2019). https://www.samsunghealthcare.com/en Accessed on 27.02.2019.

[88] Mike Schuster and Kuldip K Paliwal. 1997. Bidirectional recurrent neural networks. *IEEE Transactions on Signal Processing* 45, 11 (1997), 2673–2681.

[89] Ghufran Shafiq, Sivanagaraja Tatinati, Wei Tech Ang, and Kalyana C Veluvolu. 2016. Automatic identification of systolic time intervals in seismocardiogram. *Scientific reports* 6 (2016), 37524.

[90] Ghufran Shafiq, Sivanagaraja Tatinati, and Kalyana C Veluvolu. 2016. Automatic annotation of peaks in seismocardiogram for systolic time intervals. In *2016 38th Annual International Conference of the IEEE Engineering in Medicine and Biology Society (EMBC)*. IEEE,

2672–2675.
[91] Takunori Shimazaki, Shinsuke Hara, Hiroyuki Okuhata, Hajime Nakamura, and Takashi Kawabata. 2014. Cancellation of motion artifact induced by exercise for ppg-based heart rate sensing. In *2014 36th Annual International Conference of the IEEE Engineering in Medicine and Biology Society*. IEEE, 3216–3219.
[92] Szymon Sieciński and Paweł Kostka. 2017. Determining Heart Rate Beat-to-Beat from Smartphone Seismocardiograms: Preliminary Studies. In *Conference on Innovations in Biomedical Engineering*. Springer, 133–140.
[93] Huynh Nguyen Phan Sinh, Rajesh K. Balan, JeongGil Ko, and Youngki Lee. 2019. VitaMon: Measuring Heart Rate Variability Using the Smartphone Front Camera. In *Proceedings of the ACM Conference on Embedded Networked Sensor Systems (SenSys) '19*. ACM.
[94] SM-24 Accessed on 29.02.2019. COM-14646 - SparkFun Electronics. (Accessed on 29.02.2019). https://www.sparkfun.com/products/11744
[95] raspberry pi 3 b+ Sparkfun, 14643. 2019. Raspberry Pi 3 B. (2019). https://www.sparkfun.com/products/14643
[96] sm-24 Sparkfun, 11744. 2019. Geophone - SM-24. (2019). https://www.sparkfun.com/products/11744
[97] JA Stankovic, Q Cao, T Doan, L Fang, Z He, R Kiran, S Lin, S Son, R Stoleru, and A Wood. 2005. Wireless sensor networks for in-home healthcare: Potential and challenges. In *High confidence medical device software and systems (HCMDSS) workshop*, Vol. 2005.
[98] Isaac Starr, AJ Rawson, HA Schroeder, and NR Joseph. 1939. Studies on the estimation of cardiac ouptut in man, and of abnormalities in cardiac function, from the heart's recoil and the blood's impacts; the ballistocardiogram. *American Journal of Physiology-Legacy Content* 127, 1 (1939), 1–28.
[99] A. Taebi, A. J. Bomar, R. H. Sandler, and H. A. Mansy. 2018. Heart Rate Monitoring During Different Lung Volume Phases Using Seismocardiography. In *SoutheastCon 2018*. 1–5.
[100] Brian E. Taebi, Amirtaha and Solar, Andrew J. Bomar, Richard H. Sandler, and Hansen A. Mansy. 2019. Recent Advances in Seismocardiography. *Vibration* 2, 1 (2019), 64–86. DOI: https://doi.org/10.3390/vibration2010005
[101] Chihiro Takano and Yuji Ohta. 2007. Heart rate measurement based on a time-lapse image. *Medical engineering & physics* 29, 8 (2007), 853–857.
[102] Kouhyar Tavakolian. 2016. Systolic time intervals and new measurement methods. *Cardiovascular engineering and technology* 7, 2 (2016), 118–125.
[103] Kouhyar Tavakolian, Brandon Ngai, Andrew P Blaber, and Bozena Kaminska. 2011. Infrasonic cardiac signals: Complementary windows to cardiovascular dynamics. In *2011 Annual International Conference of the IEEE Engineering in Medicine and Biology Society*. IEEE, 4275–4278.
[104] Galen S Wagner. 2001. *Marriott's practical electrocardiography*. Lippincott Williams & Wilkins.
[105] Edward Jay Wang, Junyi Zhu, Mohit Jain, Tien-Jui Lee, Elliot Saba, Lama Nachman, and Shwetak N Patel. 2018. Seismo: Blood pressure monitoring using built-in smartphone accelerometer and camera. In *Proceedings of the 2018 CHI Conference on Human Factors in Computing Systems*. ACM, 425.
[106] Chenxi Yang, Sunli Tang, and Negar Tavassolian. 2016. Annotation of seismocardiogram using gyroscopic recordings. In *2016 IEEE Biomedical Circuits and Systems Conference (BioCAS)*. IEEE, 204–207.
[107] Chenxi Yang, Sunli Tang, and Negar Tavassolian. 2017. Utilizing gyroscopes towards the automatic annotation of seismocardiograms. *IEEE Sensors Journal* 17, 7 (2017), 2129–2136.
[108] Frank G Yanowitz. 2012. Introduction to ECG interpretation. *LDS Hospital and Intermountain Medical Center* (2012).
[109] Frank G. Yanowitz. Accessed on Dec.06 2019. ECG Learning Center. (Accessed on Dec.06 2019). https://ecg.utah.edu/
[110] Jingting Yao, Srini Tridandapani, Carson A Wick, and Pamela T Bhatti. 2017. Seismocardiography-based cardiac computed tomography gating using patient-specific template identification and detection. *IEEE journal of translational engineering in health and medicine* 5 (2017), 1–14.
[111] Vahid Zakeri, Alireza Akhbardeh, Nasim Alamdari, Reza Fazel-Rezai, Mikko Paukkunen, and Kouhyar Tavakolian. 2016. Analyzing seismocardiogram cycles to identify the respiratory phases. *IEEE Transactions on Biomedical Engineering* 64, 8 (2016), 1786–1792.
[112] J. M. Zanetti and D. M. Salerno. 1991. Seismocardiography: a technique for recording precordial acceleration. (May 1991), 4–9. DOI: https://doi.org/10.1109/CBMS.1991.128936
[113] John M Zanetti and Kouhyar Tavakolian. 2013. Seismocardiography: Past, present and future. In *2013 35th Annual International Conference of the IEEE Engineering in Medicine and Biology Society (EMBC)*. IEEE, IEEE Engineering in Medicine and Biology Society (EMBC), 7004–7007.
[114] Zephyr 2019. The leading Insights-as-a-Service enterprise solution for Life Sciences companies. (2019). https://zephyrhealth.com/ Accessed on 27.02.2019.
[115] Qi Zhang, Qingtian Wu, Yimin Zhou, Xinyu Wu, Yongsheng Ou, and Huazhang Zhou. 2017. Webcam-based, non-contact, real-time measurement for the physiological parameters of drivers. *Measurement* 100 (2017), 311–321.
[116] Mingmin Zhao, Shichao Yue, Dina Katabi, Tommi S. Jaakkola, and Matt T. Bianchi. 2017. Learning Sleep Stages from Radio Signals: A Conditional Adversarial Architecture. In *Proceedings of the 34th International Conference on Machine Learning (Proceedings of Machine Learning Research)*, Doina Precup and Yee Whye Teh (Eds.), Vol. 70. PMLR, International Convention Centre, Sydney, Australia, 4100–4109.